DTU Construct
Department of Mechanical Engineering

Evaluation of methods to determine the circulating refrigerant composition in hydrocarbon mixtures heat pumps: influence of oil solubility and inhomogeneous flow

Master Thesis

Evaluation of methods to determine the circulating refrigerant composition in hydrocarbon mixtures heat pumps: influence of oil solubility and inhomogeneous flow

Master Thesis
1st February, 2026

By
Virginia Natonek

Cover photo: Magda Ehlers, 2019
Published by: DTU, Department of Mechanical Engineering, 403, 2800 Kgs. Lyngby Denmark
www.construct.dtu.dk

Approval

This thesis has been prepared over five months at the Section for DTU Thermo, Department of Mechanical Engineering, at the Technical University of Denmark, DTU, in partial fulfilment for the degree Master of Science in Engineering, MSc Eng. This thesis counts for 30 ECTS and it has been running starting from the 1st September 2025.

The complete set of models implemented and employed in this study is openly available in the following GitHub repository ”Thesis-Zeotropic-Mixtures” [1].

This research was partly funded by The Energy Technology Development and Demonstration Programme (EUDP) under the project title ” HP2MIX - High Performance Heat Pumps with Zeotropic Mixtures”, case no. 640242-533761.

Virginia Natonek - s226663

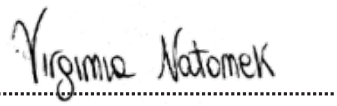

Signature

01/02/206

Date

Abstract

This research investigates different numerical approaches for determining the circulating composition in heat pump systems operating with zeotropic mixtures in the presence of compressor lubricating oil. Particular attention is given to composition shifts arising from two key mechanisms: the preferential solubility of refrigerant components in the lubricant and liquid hold-up in two-phase regions due to vapour–liquid slip. An assessment of in-situ composition measurement techniques indicates that density and speed of sound (SoS) measurements in the gaseous phase are highly sensitive to variations in mixture composition, making them suitable for detecting compositional changes. In the case that no experimental data is available, the change in mixture composition can be quantified using a thermodynamic framework based on vapour-liquid equilibrium (VLE) conditions, indicating that the fugacity of each component in the liquid-phase must equal its fugacity in the vapour-phase. The model combines Peng Robinson equation of state (modelling the vapour-phase) and NRTL activity coefficient model (for the liquid-phase). The results demonstrate that oil–refrigerant interactions and phase-distribution effects can induce measurable shifts in the circulating composition relative to the charged mixture. For a nominal charge of 55% Propane and 45% Isopentane, preferential solubility in PAG 68 shifted the effective composition to 56.2% Propane. Incorporating local composition modelling for heat exchanger hold-up results in a final circulating composition of 57.9% Propane. This total net shift of +3.06% leads to an increase of operating pressures and volumetric performance metrics, while its impact on the overall cycle efficiency was found to be comparatively moderate.

Acknowledgements

Virginia Natonek, Thesis Author, MSc Sustainable Energy Technologies, specializing in Thermal Energy Conversion and Storage, DTU

Jonas Kjær Jensen, Thesis Supervisor, Technical University of Denmark, Nils Koppels Alle, Building 403, 2800 Kgs. Lyngby, Denmark

Wiebke Brix Markussen, Thesis Supervisor, bDanish Technological Institute, Gregersensvej, 2630 Taastrup, Denmark

Roger Padulles I Sole, Thesis Supervisor, Technical University of Denmark, Nils Koppels Alle, Building 403, 2800 Kgs. Lyngby, Denmark

Preface

This thesis acknowledges the use of generative artificial intelligence (AI) tools during its preparation. Specifically, AI assistance was employed for the following purposes:

- Supporting code development and debugging
- Assisting with language refinement and proper phrasing of the manuscript

All AI-generated content has been carefully reviewed, verified, and integrated by the author to ensure accuracy and alignment with the research objectives. The intellectual contributions, research design, data analysis, and conclusions presented in this work remain entirely the responsibility of the author.

Contents

1 Nomenclature

Subscripts

0	At standard conditions
c	At critical properties
charge	Charged composition
circ	Circulating composition
ds	Downstream conditions
eff	Effective composition after oil-retention
exp	Experimental
hold-up	Liquid hold-up in the two-phase region of the heat exchangers
i, j	Components in the mixture
L	Liquid phase of refrigerant
mix	Mixture properties
oil	Oil properties
r	Refrigerant properties
sat	Saturation properties
shift	Difference between charged and circulating composition
us	Upstream conditions
V	Vapour phase

Greek Symbols

α	Soave function [-]
α_j	Void fraction component j [-]
δ	Difference between local composition and local composition at equilibrium [-]
δX_i	Uncertainty of measured variable [-]
γ	Activity coefficients [-]
Λ	Binary interaction parameters [-]
ω	Acentric factor [-]
ω_{oil}	Oil concentration (mass ratio) [-]
ϕ	Fugacity coefficient [Pa]
ρ	Density [kg/m^3]
τ	Adjustable interaction parameter of Λ [-]
ξ	NRTL non-randomness coefficient [-]

Variables

a, b	Peng–Robinson EoS parameters [-]
A	Area heat exchangers [m^2]
A, B	Peng–Robinson EoS parameters [-]
$C_{i,j}$	Local composition [kg/kg]
COP	Coefficient of performance [-]
D	Diameter [m]
$D_{i,j}$	Local composition at equilibrium [kg/kg]
f_i^L	Fugacity of the refrigerant in the liquid phase [Pa]
f_i^V	Fugacity of the refrigerant in the vapour phase [Pa]
h	Specific enthalpy [kJ/kgK]
k_{ij}	Binary interaction parameter [-]

M	Mass [kg]
m	Peng–Robinson EoS parameter [-]
P	Pressure [Pa] or [kPa]
P_e	Poynting correction factor [-]
R	Model output of the uncertainty analysis [-]
R_m	Universal gas constant [m^3 Pa/K]
S	Slip ratio [-]
T	Temperature [K]
v	Liquid molar specific volume [m^3/mol]
VHC	Volumetric heat capacity [kJ/m^3]
x	Liquid mass fraction [-]
x_i	Mole fraction in liquid phase of component i [-]
y	Vapour mass fraction [-]
y_i	Mole fraction in vapour phase [-]
z	Concentration [-]
Z	Compressibility factor [-]

2 Introduction

When using zeotropic mixtures in heat pumps applications, the circulating composition often deviates from the nominally charged mixture [2]. Existing approaches to determine circulating composition are distinguished between ex-situ methods and in-situ methods. Gas chromatography (GC) is the most widely used ex-situ measurement technique given the high accuracy and the ability of directly measuring composition [3]. However, GC is costly, and requires invasive sampling and time consuming analysis [4]. In contrast, in-situ methods are cost-effective and non-invasive. They typically rely on measuring fluid properties or system performance and then determining the circulating composition through back-calculation with a suitable equation of state (EoS). According to the Gibbs phase rule, a single-phase binary mixture requires three independent intensive properties to uniquely define its thermodynamic state. While pressure and temperature are commonly measured, these alone are insufficient to resolve the mixture composition. Therefore, a third property-such as density, enthalpy, or vapour quality, may be incorporated, like in the methods proposed by Haider & Albel [3]. After measuring the selected properties, the procedure consists of iteratively adjusting the mass fraction until the measured property aligns with the value predicted by the EoS [4]. Haider & Elbel [3] showed that pressure-temperature-based methods (PTh and PTx) tended to underestimate the circulating composition by 0.02-0.08, while the density-based PTD liquid method overestimated it by 0.08-0.12. In comparison, the ex-situ GC method provided consistent accuracy within $\pm$0.02, even in the presence of oil, although at the cost of requiring sampling. Importantly, the discrepancies between in-situ and ex-situ techniques were found to shift the predicted peak COP by up to $\pm$3%, underlining the need for calibration of in-situ methods against a reliable reference to ensure their practical applicability in heat pump systems. Brendel et al. [4] investigated six different composition determination methods, all non-invasive, five of which were conducted during system operation. The names of the six methods applied to binary and ternary mixtures are the following: evaporator inlet temperature, dew point temperature, density, speed of sound, condenser energy balance, and resting pressure. The density-based method was demonstrated to be the most accurate with an average deviation from the charged composition of less than 0.01 for all binary blends. The speed of sound-based method showed good performance with a deviation up to 0.03, but showed systematic error for the R-32 mixtures. The evaporator inlet temperature method showed a good balance between cost-effectiveness and accuracy of the properties predictions, while the resting pressure- and energy balance-based methods were shown to be less reliable due to higher sensitivity to uncertainties and operating conditions. When no experimental data is available, the behaviour of refrigerants-oil mixtures can be modelled using thermodynamic models. In this case it is important to distinguish the two main mechanisms that drive composition shift [5]. First, when a zeotropic mixture undergoes phase change, the vapour and liquid phases continuously differ in composition: the vapour becomes enriched in the more volatile component, while the liquid retains more of the less volatile one [2]. Because the vapour and liquid phases travel at different velocities, the slip ratio deviates from unity, leading to re-distribution and liquid hold-up in the two-phase region of the heat exchangers [5]. The study made by Bao & Zhao [5] on the influence of system parameters on the composition shift for a mixture of Isobutane and Pentane, showed that the enrichment in the most volatile component of about 1% , is sufficient to considerably decrease the system performance [6]. Second, the refrigerant components exhibit different solubilities in the lubricating oil. Depending on the

refrigerant-to-oil mass ratio, this can significantly alter the effective circulating composition [7]. In addition to composition shift due to inhomogeneous flow, the presence of oil in the refrigerant cycle introduces further complexity in determining the circulating composition. Oil dissolves refrigerants to different extents, leading to preferential solubility that shifts the effective mixture composition. Studies by Lebreton & Vuillame [8] have shown that oil concentration strongly affects the speed of sound in the liquid phase, with its influence depending not only on composition but also on temperature and pressure. Moreover, oil can modify boiling and condensation curves, increase viscosity and pressure losses, and reduce the efficiency of the cycle by raising the ratio of condenser to evaporator saturation pressure. From a measurement perspective, oil complicates both calibration and validation procedures. For example, density is only weakly sensitive to oil concentration, while speed of sound is more strongly correlated and can therefore serve as an indirect oil indicator. This strong dependency between mixture's properties and the presence of oil in the system highlights the need for models that explicitly incorporate oil-refrigerant interactions. The effect of the oil on mixture properties can be captured by integrating mixing rules to describe the refrigerant-oil interactions, as suggested by Mermond et al. [9], who proposes to treat the refrigerant mixture and oil as a multi-component system, taking into account the solubility of each refrigerant component in the oil. While composition shift has been a phenomenon widely studies by the scientific community, previous works have predominantly addressed it from either a purely thermodynamic equilibrium point of view or through isolated experimental observations, without fully resolving the combined drivers responsible for mixture composition variations. In particular, the combined influence of refrigerant–oil interactions and slip-induced phase re-distribution on the circulating composition has received limited attention. This present work aims at addressing these gaps by providing a mechanisms-oriented and measurement-integrated approach for hydrocarbon zeotropic mixtures.

3 Methodology

This chapter outlines the methodological framework adopted to investigate composition shift in zeotropic mixtures. The research is guided by a main research question, which is then supported by multiple sub-questions addressing the underlying mechanisms, the sensitivity and accuracy of the methods, the validity of property models, and the implications for system performance.

How can the circulating composition of hydrocarbon mixtures in heat pumps be determined, considering the effects of thermodynamic non-ideality, oil–refrigerant interactions, and two-phase flow dynamics?

The main research question is supported by the following sub-questions:

1. How sensitive are vapour–liquid equilibrium properties of the selected binary mixtures to composition changes?
2. How does the presence of compressor lubricant oil affect the circulating composition and thermophysical properties under given heat-pump operating conditions?
3. How do vapour–liquid slip and liquid hold-up in two-phase regions of heat exchangers contribute to deviations between charged and circulating composition?
4. How do combined oil-induced and flow-induced composition shifts affect operating pressures, COP, and volumetric heating capacity of a heat-pump cycle?

The methodology is structured into four main parts. Firstly, the mixture components are defined, and the methods for computing their physical properties are delineated. Secondly, in-situ measurements methods are presented. These methods rely on thermodynamic property calculations and measured operating conditions in order to estimate the mixture composition during system operation, without the need for direct sampling. Thirdly, the mechanisms contributing to the mixture composition shift are analysed. The first mechanism identified is the preferential solubility of the individual refrigerant components in the compressor lubricating oil, which alters the effective circulating composition by selectively retaining certain components in the oil-rich liquid-phase. Finally, composition shift associated with liquid hold-up in the two-phase regions of heat exchangers is studied. This mechanism arises from phase separation due to velocity differences between the liquid and gaseous phase of the mixture, leading to local enrichment of components with lower volatility and a corresponding shift in the circulating composition. Together, these methods provide a comprehensive framework for predicting the circulating composition and for analysing the predominant contributors to composition shift in heat pump systems. The complete set of models implemented and employed in this study is openly available in the following GitHub repository ”Thesis-Zeotropic-Mixtures” [1].

3.1 Definition of the refrigerants-oil system

This section introduces the components of the mixture considered in this study, namely Propane, Isopentane, and the compressor lubricating oil PAG 68.

3.1.1 Propane-Isopentane mixture

The selected mixture of refrigerants is the result of a previous study which developed a multi-stage screening framework that evaluated hydrocarbons mixtures across multiple

operating scenarios. The proposed framework was then applied to a case study representing a geothermal energy facility coupled to a district heating network in Denmark. The system was analysed under five representative operating scenarios to capture variations in sink and source temperature levels, and within this framework, the mixture 55% Propane and 45% Isopentane consistently outperformed the other hydrocarbon blends. Unlike pure fluids where evaporation and condensation happen isothermally (at constant temperature), for mixtures the start and end of the evaporation process occur at the bubble- and dew-point temperatures, and vice versa for condensation (as shown in Figure 3.1). Moreover, when refrigerants mixtures are considered, two distinct groups are defined based on their phase changing process, namely azeotropes and zeotropes. When in equilibrium, azeotropes exhibit the same composition in both the liquid and vapour-phase, and they can be simplified as single component refrigerants. On the contrary, zeotropic mixtures show different vapour and liquid compositions when in equilibrium [10]. As a matter of fact, during phase change, differences in the boiling points of the mixture components lead to preferential evaporation or condensation of the individual elements [11]. Hence, the composition of the phase changing mixture evolves along the process, giving rise to a composition shift [12]. This shift is accompanied by changes in the dew- and bubble-point temperatures of the remaining mixture, causing the phase change to occur over a temperature range rather than at a single temperature [10].

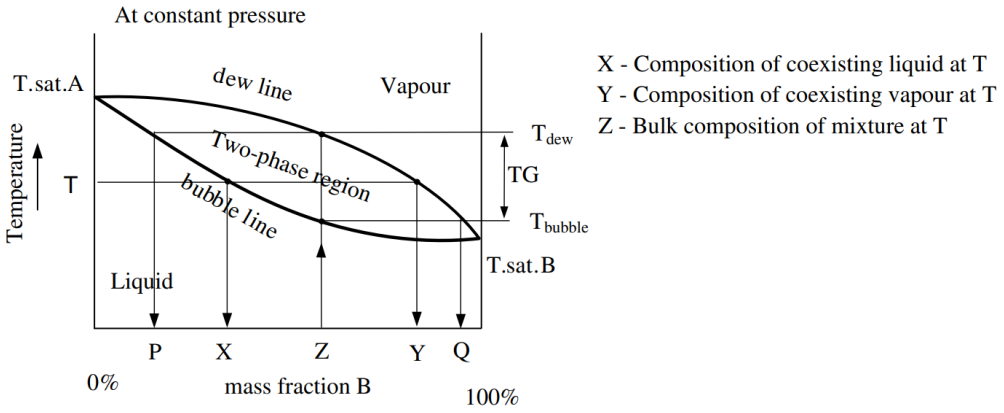

Figure 3.1: Phase changing process of a zeotropic mixture [10].

Early experimental work by Vaughan and Collins [13] provides detailed pressure–volume–temperature–composition (P–V–T–x) data for several Propane–Isopentane mixtures over a wide range of temperature and pressure values, including the two-phase and critical regions. Figure 3.2a presents the pressure–temperature phase envelopes for the mixture at different compositions, ranging from pure Propane to pure Isopentane. Each curve represents the saturation boundary of a fixed composition mixture, showing the separation between bubble- and dew-point conditions. This confirms the zeotropic nature of the mixture and highlights the non-isothermal character of phase change of Propane-Isopentane mixtures. Similarly, Figure 3.2b exhibits shows the saturation pressure as a function of mixture composition at different temperatures. The strong dependence of saturation pressure on composition demonstrates that even moderate changes in local composition could lead to noticeable variations in the thermodynamic state of the mixture. The curvature of the isotherms further reflects the non-ideal behaviour of the mixture and the dissimilar volatility of Propane and Isopentane.

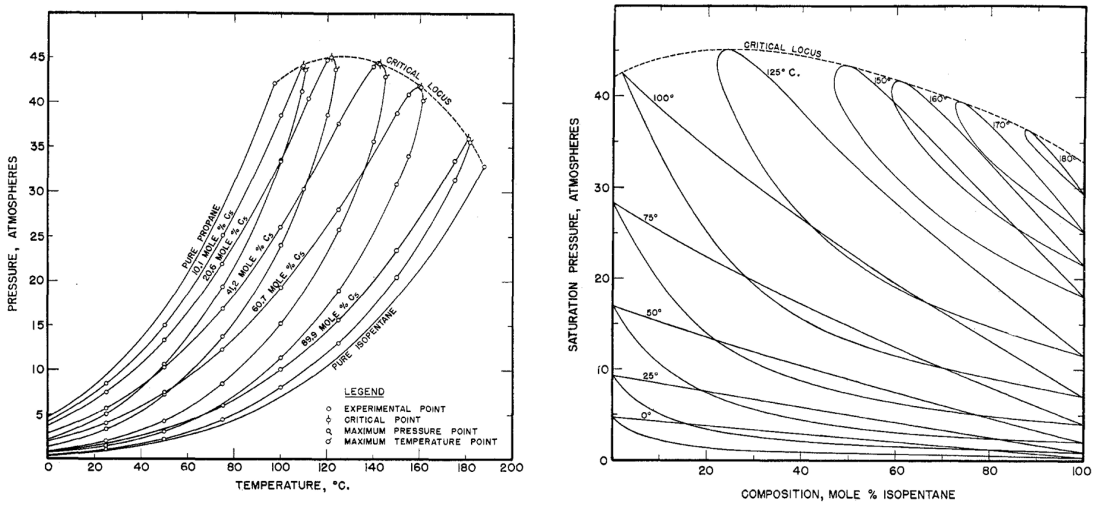

(a) Pressure vs Temperature.

(b) Pressure vs Composition.

Figure 3.2: Bubble point and dew point curves of Pressure vs Temperature (a) and Pressure vs Composition (b) [13].

3.1.2 Compressor lubricant oil

The compressor lubricant oil for used in the present study is selected to be PAG 68. PAG 68 is a synthetic and hygroscopic oil (i.e. it absorbs and binds moisture from ambient air) based on polyalkalene glycol (PAG) [14]. This oil is suitable for screw and reciprocating piston compressors, and it is recommended for the use with hydrocarbon refrigerants. According to literature, PAG 68 oil is highly resistant to dilution by hydrocarbon gases, which allows the oil to resist absorption into the refrigerant gas stream and subsequent carry over of the lubricant downstream the compressor unit [15]. Table 3.1 summarizes the properties of PAG 68 according to manufacturer specifications.

Table 3.1: Manufacturer data of PAG 68 oil [14].

Property	Value	Unit
Density at 15 °C	1044	kg/m^3
Flash point (Cleveland)	250	°C
Kinematic viscosity at 40 °C	70	mm^2/s
Kinematic viscosity at 100 °C	14	mm^2/s
Pour point	-52	°C

Considering that most manufacturers of lubricating oils provide density data only at standard conditions, as reported in Table 3.1, correlations have been developed to estimate density values over a range of different temperatures [16]. Sun et al. [17] proposes to determine the density of PAG 68 over a temperature range from 283.15 to 343/15 K at 0.1 MPa using a Tait-type equation as it follows:

$$\rho(T) = A_0 + A_1 T + A_2 T^2 + A_3 T^3 \tag{3.1}$$

where A_1, A_2, and A_3 are obtained from literature, and are proclaimed to successfully represent oil densities when compared to experimental data [17].

$$A_0 = 1371.50 \quad A_1 = -1.646 \quad A_2 = 1.54\text{E-}03 \quad A_3 = -1.91\text{E-}03$$

3.2 In-situ measurements methods of circulating composition

According to the Gibbs phase rule, a single-phase binary mixture requires three independent intensive properties to uniquely define its thermodynamic state. Although pressure and temperature are easily measured, they are insufficient to uniquely determine the mixture composition [3]. In practice, this can be solved by measuring an additional thermophysical property that is highly sensitive to mixture composition. The composition is then estimated by iteratively adjusting the mass fraction within an equation-of-state–based model, using REFPROP [18], until the calculated property matches the measured value. Figure 3.3 taken from the study of Brendel at al. [4] visually represents the methodology here presented. Information from blocks A and B can be combined to compute the quantities measured in block D, which are then compared with the corresponding measurements (block C). Alternatively, the measurements in blocks A and D may be taken as known inputs and used to determine the mixture mass fraction in block B [4].

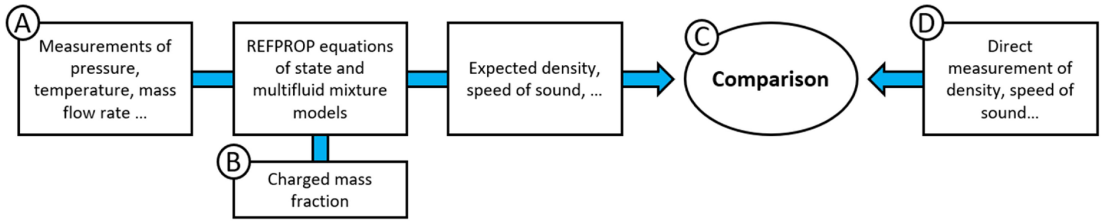

Figure 3.3: Comparison of measurements with mixture equations implemented in REFPROP [4].

In this study three different composition determination methods are analysed using density, speed of sound and enthalpy.

3.2.1 Density-based approach

The Pressure-Temperature-Density (PTD) approach allows to determine the composition of a gaseous or liquid mixture by measuring pressure (P), temperature (T), and density (D), and comparing the values with those obtained using REFPROP [3]. It is distinguished between PTD gas and PTD liquid methods. For the former, the literature recommends to measure the gas density using a PTD sensor which incorporates a microelectromechanical (MEMS) based oscillator and has a measurement uncertainty of ± 0.1 kg/m^3 [3]. Regardless the availability of the sensor, the literature underlines the novelty of the method when applied to gaseous zeotropic mixtures. However, the PTD gas method is still a valuable alternative to gas chromatography, given the lower equipment costs. The sensor used in the study has certain operational constraints, limiting its use to gaseous samples up to 1000 kPa and densities of approximately 20 kg/m^3 [3]. Under these constraints, the literature indicates placing the sensor at the compressor's suction port, while noting that the presence of the oil in the system may interfere with the system's accuracy [3]. For the PTD liquid approach, the measurements are taken when the mixture is in the liquid-phase, using a Coriolis flow meter. Brendel et al. [4] provides suggestions for the sensor location to achieve the highest accuracy of liquid density measurements. Specifically for the PTD liquid density method, the authors propose to locate the flow meter in the liquid line after the internal heat exchanger, the pressure sensor upstream of the receiver, and the thermocouple 1 m downstream of the density meter [4]. The method was also used by Zhang et al. [19], who estimated the composition of the mixture R134a/R245fa by measuring the liquid density of the mixture at the outlet of the working fluid pump using

a Coriolis mass flow meter. The function solved to find the composition is the following:

$$f(x_i) = \rho_{\text{calc}}(T, P, x_i) - \rho_{\text{exp}} \tag{3.2}$$

where x_i is treated as the unknown variable, and pressure P and temperature T are measured. For a given trial composition x_i, the corresponding density ρ_{calc} is calculated using REFPROP. The residual function $f(x_i)$ thus quantify the mismatch between the model-predicted density and the experimentally measured one ρ_{exp}.

3.2.2 Speed of sound-based approach

The speed of sound (SoS) approach exploits the strong dependence of the acoustic velocity of a fluid on its thermodynamic state and composition [20]. In practical implementations, the SoS sensor is installed inline at a location where the refrigerant is guaranteed to be in a single-phase state, typically measuring superheated vapour at the compression suction, or subcooled liquid upstream of the expansion valve [4]. The SoS is measured by quantifying the time required for an acoustic wave to propagate between a geometrically fixed transmitter and receiver, from which the speed of sound in the medium is determined [4]. The speed of sound depends on the composition of the fluids, as well on its temperature and pressure. Hence, the following measurements are required:

$$x_i = f(T, P, u) \tag{3.3}$$

These measured values are then compared against the properties calculated using REFPROP. A similar approach to the one previously presented in Equation 3.2 for the density-based approach is implemented, to iteratively find the mixture composition that allows convergence between the evaluate SoS using a mixture equation of state and the measured value.

3.2.3 Enthalpy-based approach

The pressure-temperature-enthalpy (PTh) method is based on the principle that the expansion across a throttling device is an isenthalpic process [4]. The circulating composition with the PTh approach can be calculated by assuming steady-state conditions and equal composition upstream and downstream the expansion valve. The following equations are defined for the PTh method [3]:

$$h_{\text{us}} = h_{\text{ds}} \tag{3.4}$$

$$h_{\text{us}} = h(T_{\text{us}}, P_{\text{us}}, w_{\text{us}}) \tag{3.5}$$

$$h_{\text{ds}} = h(T_{\text{ds}}, P_{\text{ds}}, w_{\text{ds}}) \tag{3.6}$$

$$z_{\text{us}} = z_{\text{ds}} \tag{3.7}$$

Literature mentions the sufficiency of a pressure measurement downstream of the valve to define the system. Nevertheless, redundancy with an additional temperature measurement can reduce the uncertainty of the composition determination [4]. This method has been already been applied by the literature [21] to the mixture R407C, which consists of three components, R134a, R32 and R125. The study also compares the estimated circulating composition obtained with the PTh method with the values acquired by gas chromatography. The comparison showed an underestimation of the molar share of R134a by 2% (absolute) compared to the alternative GC values, with temperature being the main source of uncertainty propagation [21]. As a matter of fact, an error of the temperature measurement of $\pm 0.5^{\circ}$C will reportedly result in an absolute error of $\pm$3% in the molar fraction of R134a. On the other hand, pressure errors are demonstrated to be less critical

than temperature errors. Moreover, the authors underline that the samples taken using gas chromatography are taken from the liquid returning to the refrigerant vessel and not exactly at the expansion valve or immediately downstream of the in-situ measurement point. Consequently, there might be some deviation between the composition measured by the in-situ method and the liquid samples because of the spatial dependency of the composition in zeotropic mixtures [21].

3.2.4 Uncertainty Propagation Analysis

When measuring and estimating the space-dependent composition of zeotropic mixtures, uncertainty is introduced from several sources, most importantly the sensor precision. Moreover, uncertainties arise from the REFPROP property predictions (dependent on the EOS of choice and mixture coefficients), the charging procedure, and the pressure and temperature measurements, which are not directly taken at the density or speed of sound sensors [4]. These factors inevitably introduce small errors, but the literature explains that even when accounting for all these inaccuracies, the calculated and measured compositions are usually in acceptable ranges of deviations, with discrepancy reaching 1.1% deviation [4]. Plus, the propagated uncertainty is strongly dependent on the specific components, mixture composition and operating conditions. Therefore, an extra analysis of the uncertainty propagation is performed for the selected mixture under defined operating conditions, while using the sensors accuracy provided by the literature, as the specifications of the sensors employed in the experimental setup are not yet available. Specifically the uncertainty of each method is determined by propagating the uncertainties from the sensors to the calculated quantities, under the assumption that the refrigerant mixture is oil-free [22, 3]. The uncertainty analysis is grounded to the concept that the uncertainty of a calculated result can be estimated with good accuracy using a root-sum square combination of the affects of each of the individual variables used as inputs to the model [23]. It follows that if the model output R is calculated from a measured variable X_i, the uncertainty in R is obtained by propagating the uncertainty of the inputs through governing equations using sensitivity coefficients [22]:

$$\delta R = \sqrt{\sum_i \left(\frac{\partial R}{\partial X_i} \delta X_i \right)^2} \tag{3.8}$$

Each term in Equation 3.8 thus represents the contribution made by the uncertainty in one variable, δX_i, to the overall uncertainty in the results, δR [22]. X_i is a variable with known uncertainty δX_i, so that:

$$X_i = X_i(\text{measured}) \pm \delta X_i \tag{3.9}$$

The measured uncertainties for the used sensors are summarized in Table 3.2.

Table 3.2: Measurement uncertainty for used sensors [4].

Property	Measurement Principle	Uncertainty
Temperature	K-type Thermocouple	$\pm$1.5 K
High Pressure	Piezoelectric	75 KPa absolute
Low Pressure	Piezoelectric	15 KPa absolute
Gas Density	MEMS resonator	$\pm$ 0.1kg/m^3
Liquid Density	Coriolis Sensor	$\pm$ 10kg/m^3
Liquid Sound Velocity	Wave propagation time	$\pm$0.01 m/s

The uncertainty in the sensor measurements may also be linked to the assumption that oil is present in the refrigerant mixture, potentially affecting the accuracy of the measured properties. In contrast, most studies in the literature assume the presence of an oil separator downstream of the compressor, and therefore neglect oil circulation in the system.

3.3 Thermodynamic framework for vapour-liquid equilibrium modelling

When modelling refrigerant-oil mixtures, different approaches are presented in the literature. Thermodynamic models that respect vapour-liquid equilibrium (VLE) conditions are based on equality of fugacities for each component in the mixture in both vapour and liquid-phase [24]:

$$f_i^L = f_i^V \tag{3.10}$$

The methods following this principle, are distinguished between local composition models (also known as heterogenous models), and homogenous models based on equations of state. Both require the calculation of fugacities for the vapour and liquid-phase, but the first type needs two different formulations to calculate the vapour and liquid fugacities, while the second uses the same calculation procedure for the two phases [25]. This study applies the first type of model, where the departure from ideal behaviour is described using the concept of fugacity for the vapour-phase, fugacity and Poynting effect correction for the liquid-phase, and finally activity coefficients for mixtures [24].

3.3.1 Vapour-phase fugacity and Peng-Robinson equation of state

To determine the fugacity of a mixture, an equation of state (EoS) is to be selected among the several models suggested in the literature. For this work, the Peng-Robinson (PR) cubic EoS is used, which has been identified as a well-suited equation for mixtures by different previous studies [26, 27, 28]. The PR EoS is expressed as [29]:

$$P = \frac{RT}{v-b} - \frac{a\alpha}{v(v+b)+b(v-b)} \tag{3.11}$$

where

$$a = 0.45724\frac{(R_m T_c)^2}{P_c}\alpha \tag{3.12}$$

$$b = 0.07780\frac{R_m T_c}{P_c} \tag{3.13}$$

Equation 3.11 uses two parameters, a and b, which are found using the critical properties of the vapour being modelled. The Soave α-function, which accounts for acentric factor and temperature dependence is expressed as follows [30]:

$$\alpha = \left[1 + M\left(1 - \sqrt{\frac{T}{T_c}}\right)\right]^2 \tag{3.14}$$

where M is a third parameter introduced by Martz et al. [28] and it is found using correlations with the working fluids acentric factor ω_i [31, 30]:

$$M = 0.37464 + 1.54226w_i - 0.26992w_i^2 \tag{3.15}$$

As these parameters are defined, the fugacity coefficient of a component in a mixture, $\bar{\phi}_i = f_i/y_i P$, is computed [29, 32]:

$$\ln \bar{\phi}_i = \frac{b_i}{b}(Z-1) - \ln(Z-B) - \frac{A}{2B\sqrt{2}}\left(\frac{2\sum_j x_j a_{ij}}{a} - \frac{b_i}{b}\right)\ln\left(\frac{Z+2.414\,B}{Z-0.414\,B}\right) \tag{3.16}$$

where $A = aP/(RT)^2$, $B = bP/RT$, and $Z = PV/RT$. The mixture parameters in Equation 3.16 are defined by the van der Waals mixing rules [29]:

$$a = \sum_i \sum_j x_i x_j a_{ij} \tag{3.17}$$

$$b = \sum_i x_i b_i \tag{3.18}$$

$$a_{ij} = \sqrt{a_i a_j}(1 - k_{ij}) \tag{3.19}$$

where k_{ij} is an empirically determined binary interaction coefficient characterizing the binary mixture formed by component i and component j. The value found for the Propane-Isopentane mixture is $k_{12} = k_{21} = 0.0111$, while $k_{11} = k_{22} = 0$ [33]. As also previously mentioned, the fugacity coefficient is a measure of deviation from the ideal-gas behaviour, but it can also express liquid-phase non-ideality:

$$f_i^L = x_i \gamma_i \bar{\phi}_i^L P \tag{3.20}$$

For thermodynamic equilibrium, the saturated liquid fugacity equals the saturated vapour fugacity (as described in Equation 3.10), which translates into:

$$x_i \gamma_i \bar{\phi}_i^L P = y_i \bar{\phi}_i^V P \tag{3.21}$$

In the equation a second term is integrated, the Poynting effect, P_e, which accounts for the influence of the system pressure on the liquid fugacity [34]. The Poynting effect for a ith component in a mixture is calculated:

$$P_{e,i} \approx exp\left[\frac{v_{i,l}(P - P_{\text{sat,i}})}{R_m T}\right] \tag{3.22}$$

where P is the system pressure, $P_{\text{sat,i}}$ is the saturation pressure for the pure component. When including the Poynting effect, Equation 3.20 can be re-written as:

$$f_i^L = x_i \gamma_i P_{\text{sat,i}} \bar{\phi}_i^L P_{e,i} \tag{3.23}$$

Considering that thermodynamic equilibrium is applied, and the fugacities of ith component in the liquid and vapour-phase are equal, Equation 3.21 is re-arranged to obtain an expression describing the activity coefficient γ_i:

$$\gamma_i = \frac{y_i \bar{\phi}_i^V P}{x_i P_{\text{sat,i}} \bar{\phi}_i^L P_{e,i}} \tag{3.24}$$

Activity coefficients greater than one indicate partial pressures higher than the product of the mole fraction and the saturation pressure, and strong attractions between molecules in the mixture of similar kind. On the contrary, activity coefficients less than one suggest strong attractions between unlike molecules [34, 35].

3.3.2 Liquid-phase non-ideality: NRTL activity coefficient modelling

Precisely predicting activity coefficients for binary mixtures or multi-component mixtures is very complex because the behaviour of liquid mixtures, especially those containing large molecules such as mixtures of refrigerant(s) with oil [36]. This problem could be solved by estimating activity coefficients and fitting the results to experimental VLE data for a given mixture. However, obtaining experimental data for every mixture of interest for different operational conditions would be a large and expensive task. It is therefore necessary to estimate activity coefficients from suitable models if little or no mixture data is available. In the literature, several models are proposed for accurately calculating activity coefficients, and all are based on a Gibbs energy formulation, which relates the temperature, pressure and concentration to the activity coefficients of the mixture [28]. The most used models in the literature are: Wilson [37], Heil [38], Wang and Chao [39], Tsuboka and Katayama [40], NRTL (Non-Random TwoLiquid) [41] and UNIQUAC (Universal Quasi-Chemical) [34]. The accuracy of the model depends on the appropriateness of the Gibbs energy relation. Mixture models with multiple interaction parameters may be more accurate, but they require more experimental data and computational effort [28]. Most of the aforementioned models require two or three adjustable parameters, referred to as binary interaction parameters, for each binary pair [36]. For a ternary mixture like the one investigated, six parameters are to be calculated: two for refrigerant 1 with oil, two for refrigerant 2 with oil, and two for the two refrigerants. Once the binary interaction parameters are determined for each refrigerant-oil pair, the pressure–temperature relationship of the mixture at any oil concentration can be predicted. For the present study, the non-random two-liquid (NRTL) mixture model is selected to assess the properties of the refrigerants-oil mixture, as it is the mixture model mostly used for this purpose in the literature. The NRTL theory, developed by Renon and Prausnitz [41] is based on the Scott's two-liquid theory of binary mixtures, which takes into account the non-randomness of mixing [42].

Binary mixture model For a binary mixture, the activity coefficients for the NRTL model are found by as it follows:

$$\ln(\gamma_1) = x_2^2 \left[\tau_{21} \left(\frac{\Lambda'_{21}}{x_1 + x_2 \Lambda'_{21}} \right)^2 + \frac{\tau_{21} \Lambda'_{21}}{(x_1 \Lambda'_{21} + x_2)^2} \right] \tag{3.25}$$

$$\ln(\gamma_2) = x_1^2 \left[\tau_{12} \left(\frac{\Lambda'_{12}}{x_2 + x_1 \Lambda'_{12}} \right)^2 + \frac{\tau_{21} \Lambda'_{12}}{(x_2 \Lambda'_{12} + x_1)^2} \right] \tag{3.26}$$

where τ_{12} and τ_{21} are adjustable parameters, found as it follows:

$$\tau_{12} = \Delta\lambda_2 / R_m T \tag{3.27}$$

$$\tau_{21} = \Delta\lambda_1 / R_m T \tag{3.28}$$

and Λ'_{12} and Λ'_{21} are obtained from:

$$\Lambda'_{12} = \exp(-\xi\tau_{12}) \tag{3.29}$$

$$\Lambda'_{21} = \exp(-\xi\tau_{21}) \tag{3.30}$$

In Equation 3.25 and Equation 3.26, the parameter ξ is an empirical constant independent of temperature and it accounts for the non-randomness of the liquid solutions [41]. When this parameter is zero, the solution is said to be completely random. For refrigerant-oil mixtures, Martz et al. [28] suggests to use ξ = 0.5 to obtain the best results. However, for the mixture Propane-oil, Sun et al. [17] indicates to consider ξ = 0.6, which is thus used as input to the NRTL model describing the blend.

Multi-components mixture model The equations for binary solutions (see Equation 3.25 and Equation 3.26) can be generalized to solutions containing any number of components [41]:

$$\ln(\gamma_i) = \frac{\sum_{j=1}^{n} \Lambda_{ji}\, \tau_{ji}\, x_j}{\sum_{k=1}^{n} \Lambda_{ki}\, x_k} + \sum_{j=1}^{n} \frac{\Lambda_{ij}\, x_j}{\sum_{k=1}^{n} \Lambda_{kj}\, x_k} \left(\tau_{ij} - \frac{\sum_{k=1}^{n} \Lambda_{kj}\, \tau_{kj}\, x_k}{\sum_{k=1}^{n} \Lambda_{kj}\, x_k} \right) \tag{3.31}$$

$$(\Lambda_{ij})_{i \neq j} = \exp(-\xi\, \tau_{ij}), \qquad (\Lambda_{ij})_{i=j} = 1 \tag{3.32}$$

$$(\tau_{ij})_{i \neq j} = \frac{\Delta\lambda_{ij}}{R_m T}, \qquad (\tau_{ij})_{i=j} = 0 \tag{3.33}$$

The lambda parameters ($\Delta\lambda_{ij}$ and $\Delta\lambda_{ji}$), quantifying the difference in interaction energy between unlike and like molecular pairs and are essential for quantifying the non-ideality of liquid mixtures, are found through a regression procedure [28]. Silverman & Tassios [43] compared ten different objective functions in the regression of VLE data for 247 binary systems and found the regression driven by the objective function:

$$Q = \sum_{i=1}^{N} \left(\frac{P_{\text{exp}} - P_{\text{model}}}{P_{\text{exp}}} \right)^2 \tag{3.34}$$

to be the most accurate in predicting results. The function measures the deviation between experimental data and model predictions in terms of pressure. Moreover, the relative squared error is demonstrated to be superior to simple squared-error method because it ensures consistent weighting across the entire pressure and composition range and is not biased by high-pressure data [28]. Although the overall structure of the mixture model and the objective function used for parameter regression remain consistent, different binary pairs were analysed using different modelling approaches and assumptions. The choice of the specific procedure is mainly adapted to the characteristics of each pair and are introduced in the subsequent subsections Ultimately, to link the oil-refrigerant equilibrium analysis with the system-level circulating-composition model, an effective refrigerant composition is computed by mass-weighting the vapour and liquid-phase refrigerant compositions according to the vapour fraction:

$$z_{\text{eff},i} = (1 - X)\, x_i + X\, y_i \tag{3.35}$$

where X is the vapour fraction of the mixture at a given temperature and pressure conditions, x_i is the mass fraction of a refrigerant component i in the liquid-phase, and y_i is the mass fraction of the component in the vapour-phase.

3.3.3 Propane-Oil

When experimental data is available, the binary interaction coefficients can be determined directly through regression of the data, as shown in Figure 3.4. The procedure starts by introducing some guessed initial values of binary parameters for the NRTL model. Experimental data for Propane-PAG68 (see Table 4.2) consisting of pressure, temperature and mixture composition values, obtained from literature is then used as input [17]. For each data point, an inner calculation is performed where the activity coefficients of the pair in the liquid-phase is first evaluated, and then used to compute fugacity coefficients of the liquid and vapour-phase, assuming that the vapour-phase consists exclusively of Propane, due to the negligible vapour pressure of the oil [44]. The calculated equilibrium pressure is then determined by enforcing equality between vapour and liquid-phase fugacities of the refrigerant. This procedure is repeated for all experimental data points in the dataset. Once the inner loop is completed, Equation 3.34 is used to minimize the deviations between calculated and experimental pressures.

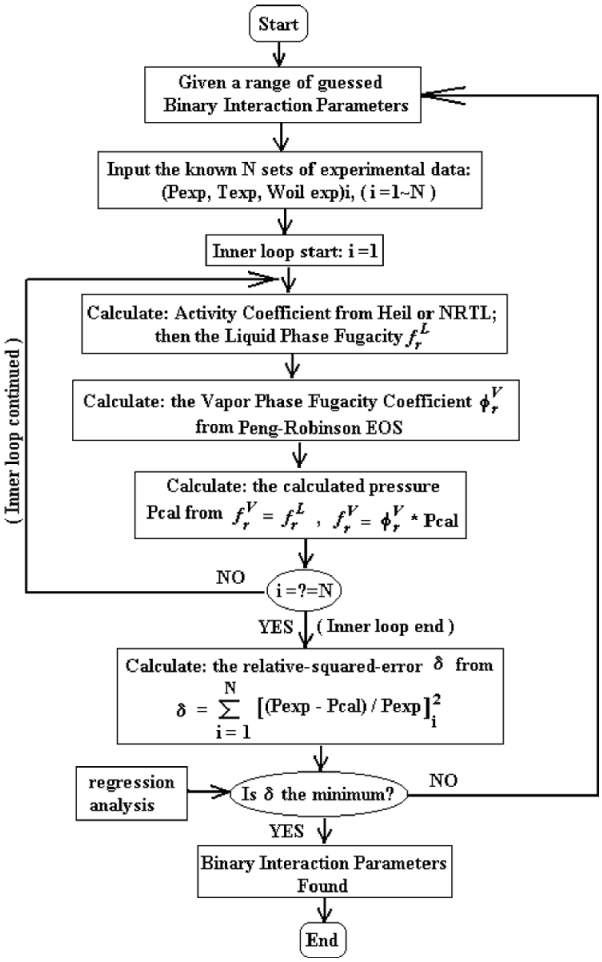

Figure 3.4: Calculation scheme for binary interaction parameters when experimental data is available [36].

3.3.4 Isopentane-Oil

In the case that no experimental data is available for the mixture studied, like for the case of Isopentane-PAG 68, the literature proposes an alternative methodology which relates the binary parameters to physical characteristics of refrigerants that are readily

available. Specifically, Fleming et al. [36] analysing data for the mixtures R22/SW46 and R134a/SW46, where SW46 oil is a synthetic polyol ester, demonstrated that the deviations from ideal behaviour for the refrigerant-oil mixtures depends on the molecular weight ratio of oil to refrigerant, which, by influencing the binary parameters and thus the activity coefficient, contributes to the deviation [36]. Similarly, the critical temperature T_c, which then combined with the universal gas constant R forms the dimensionless group $\Delta\lambda/R_m T_c$, can be used. Considering the fact that the critical properties of the oil are usually not readily available, the critical temperature of the refrigerant is used in the coefficients formulation. For $\Delta\lambda_{12}/R_m T_{c,r}$ < 1.4, $\Delta\lambda_{12}$ is expressed as:

$$\left(\frac{MW_{\text{oil}}}{MW_r}\right) = 2.6165\left(\frac{\Delta\lambda_{12}}{RT_{c,r}}\right) + 7.4682 \tag{3.36}$$

while $\Delta\lambda_{12}/RT_{c,r} \geq$ 1.4, $\Delta\lambda_{12}$ is:

$$\left(\frac{MW_{\text{oil}}}{MW_r}\right) = 2.2102\left(\frac{\Delta\lambda_{12}}{RT_{c,r}}\right) - 0.2274 \tag{3.37}$$

For $\Delta\lambda_{21}$:

$$\left(\frac{MW_{\text{oil}}}{MW_r}\right) = -2.3873\left(\frac{\Delta\lambda_{21}}{RT_{c,r}}\right)^2 - 7.2132\left(\frac{\Delta\lambda_{21}}{RT_{c,r}}\right) + 1.3211 \tag{3.38}$$

where subscripts 1 and 2 stand for refrigerant and oil, respectively. The molecular weight of oil may be obtained from the oil manufacturer or estimated from equations suggested by Conde at. [16]. For this correlation to be valid, the authors suggest to apply it to refrigerant-oil mixtures that have molecular weight ratios in the range of 2.9-8.1 [36], which makes it applicable to the mixture Isopentane-oil.

3.3.5 Propane-Isopentane

For the pair Propane-Isopentane, no readily available experimental data is found, and synthetic data is generated based on phase equilibrium calculations. The thermophysical properties of the mixture are obtained using REFPROP and adjusted using a constant binary interaction parameter, k_{ij} obtained from the literature [33]. The procedure to determine the effective circulating composition is the same used for the Propane-oil mixture, using the generate data rather than experimental data.

3.3.6 Effects of oil on the VLE properties of the ternary mixture

Once the thermodynamic framework for the ternary mixture (Propane–Isopentane–Oil) is fully defined and the binary interaction parameters for all pairs are obtained, the effect of oil on the mixture thermodynamic properties at equilibrium is analysed. The analysis follows the methodology proposed by Fleming et al. [36]. The approach was developed for predicting the equilibrium pressure conditions at constant temperature, and for predicting the bubble-point temperature at constant pressure, as a function of varying oil concentration in the circuit. The constant pressure and temperature values are taken from previous simulations of a single-stage heat pump cycle with internal heat exchanger and represent the operational conditions of the refrigerants mixture (without oil) at the suction line of the compressor.

Equilibrium pressure predictions at constant temperature

First, the effects of oil on the mixture equilibrium pressure is examined at fixed temperature and liquid-phase composition. The calculations follow the procedure presented by Fleming et al. [36], which aims at iteratively calculating the pressure enforcing equality between liquid-phase and vapour-phase fugacities. An initial pressure guess is iteratively updated until convergence is achieved.

Bubble point temperature predictions at constant pressure
The model is also extended to evaluate the effects of oil presence on the bubble-point temperature of the mixture at constant pressure. The saturation temperature in the presence of oil is in fact expected to be higher than that of oil-free single fluid or refrigerants blends. The difference between the two temperatures is defined as ”temperature rise” [36]. The calculation procedure to obtain the saturation temperature of the oil-rich mixture is similar to the one previously presented for pressure predictions at constant temperature, but with the roles of temperature and pressure switched. For a given pressure and liquid-phase composition, the bubble point temperature is computed iteratively. At each iteration step, a guess value for the temperature is assumed, activity coefficients and fugacity coefficients are estimated, and the resulting equilibrium pressure is calculated. The bubble-point temperature corresponds to the temperature at which the calculated pressure matches the enforced system pressure. The procedure hence includes a root-finding algorithm, where the residual is defined as the difference between the calculated pressure and the prescribed one as input.

Model validation and comparison with empirical correlation
To validate the temperature predictions in the presence of oil, the model results are compared against the empirical correlation proposed by Fleming et al. [36] (originally attributed to Thome [45]), which expresses the bubble-point temperature as an explicit function of pressure and oil concentration w_{oil}, and is expressed as it follows [45]:

$$T = \frac{A(w_{\text{oil}})}{ln(P_{\text{MPa}}) - B(w_{\text{oil}})} \tag{3.39}$$

where P_{MPa} is the vapour pressure in MPa and $A(w_{\text{oil}})$ and $B(w_{\text{oil}})$ are functions of the oil concentration, and are defined as it follows:

$$A(w_{\text{oil}}) = a_0 + a_1 w_{\text{oil}} + a_2 w_{\text{oil}}^3 + a_3 w_{\text{oil}}^5 + a_4 w_{\text{oil}}^7 \tag{3.40}$$

$$B(w_{\text{oil}}) = b_0 + b_1 w_{\text{oil}} + b_2 w_{\text{oil}}^3 + b_3 w_{\text{oil}}^5 + b_4 w_{\text{oil}}^7 \tag{3.41}$$

The empirical constants when oil is present are [36]:

$$a_1 = 182.52 \quad a_2 = -724.21 \quad a_3 = 3868.0 \quad a_4 = -5268.9$$
$$b_1 = -0.72212 \quad b_2 = 2.3914 \quad b_3 = -13.779 \quad b_4 = 17.066$$

where a_0 and b_0 represent the baseline saturation behaviour of the oil-free mixture. These constants are estimated by least-square fitting pressure values predicted by the correlation to refrigerants-dependent data (obtained using REFPROP) over a defined temperature range.

3.4 Local Composition Modelling

For a more accurate and comprehensive analysis of the impact of composition shift on the system, it is notable to investigate not only the circulating composition but also the local composition within the heat exchangers. In a two-phase flow where both liquid and gas are present, local composition is associated with a spatial position parameter z which is a static concept described by Euler method, whereas flow composition is a dynamic concept related to time and described by the Lagrange method [46]. In general, the gas phase travels at a higher velocity than the liquid-phase. When working with mixtures, the difference in composition between liquid and gas phase (as shown in Figure 3.5) results in a continuous redistribution of the individual components between the two phases. This leads to spatial variations in mixture composition along the flow path, which are mainly governed by phase equilibrium and phase hold-up effects.

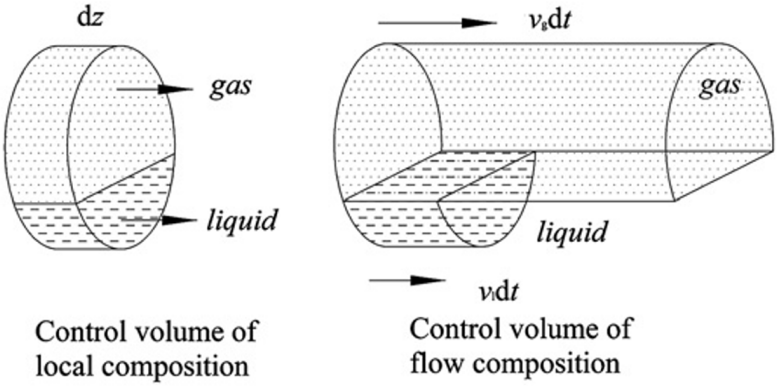

Figure 3.5: Control volume of local composition and flow composition [46].

Local composition shifts influence the mixture composition, which might alter heat transfer performance and may result in off-design operating conditions [47]. Different studies simulated the change in local composition of zeotropic mixtures in refrigeration and heat pumps systems. Youbi-Idrissi et al. [48] proposes a local composition model of a water-to-water heat pump using R407c by adopting a modular approach. The overall model consists of combining elementary models for each of the system component, i.e. compressor, condenser, evaporator and receiver, to then evaluate the performance of the machine, as well as the local temperature and heat transfer coefficients along the heat exchangers and the local composition of the mixture components at each point of the circuit. Jeong et al. [47] explored local composition shift within the evaporator under various experimental conditions, including charge composition, compressor speed, and heat source temperature. An important finding of Xu et al. [46] is that local composition shift cannot be described by equilibrium thermodynamics alone. Instead, it depends strongly on the void fraction and slip ratio, which determine the relative volumetric contributions of the gas and liquid-phases. To account for these non-equilibrium effects, a distributed two-phase flow model is adopted, in which the local phase distribution is evaluated along the heat exchangers. The two heat exchangers are assumed to be concentric double pipe heat exchangers with the dimensions and geometry presented by one of the applications found in the literature [36]. The inputs are summarized in Table 3.3.

Table 3.3: Size of the heat exchangers and mixture charge [49].

	Definition	Parameter	Unit
Inner diameter	D_i	8.0	mm
Working fluid charge	M_{charge}	0.35	kg
Evaporator area	A_{evap}	0.1864	m^2
Condenser area	A_{cond}	0.4722	m^2

Both the heat exchangers are divided into three zones, including subcooled zone, two-phase zone and superheated zone. On this basis, the two-phase zone is discretized into N control volumes, numbered from 1 to N, as displayed in Figure 3.6.

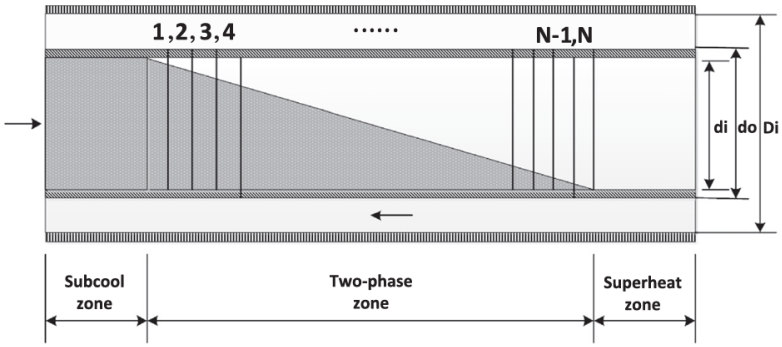

Figure 3.6: Discretization in control volumes in the evaporator and condenser [49].

The method is primarily based on the conservation of mass and it assumes that the composition of single-phase zeotropic mixture is uniform [49]. Disregarding the effects of lubricating oil in the system , the circulating composition is calculated as it follows:

$$Z_{\text{cir}} = \frac{Z_j M_{\text{charge}} - \sum M_{\text{j,hold-up}}}{M_{\text{charge}} - \sum M_{\text{hold-up}}} \tag{3.42}$$

where Z_j is the charge of the low-boiling point working fluid, M_{charge} is the working fluid charge and $M_{\text{j,hold-up}}$ and $\sum M_{\text{hold-up}}$ are the total hold-up mass and the low-boiling point working fluid hold-up mass of evaporator in the two phase zone [49]. $M_{\text{j,hold-up}}$ and $\sum M_{\text{hold-up}}$ are estimated:

$$\delta M_j = \delta V_j(\rho_{V,j}\alpha_j + \rho_{L,j}(1-\alpha_j)) \tag{3.43}$$

where δM_j describes the mass of the jth control volume, while the mass of the ith component in the mixture in the $j$the control volume is calculated with the following equation:

$$\delta M_{i,j} = \delta V_j(y_{i,j}\rho_{V,j}\alpha_j + x_{i,j}\rho_{L,j}(1-\alpha_j)) \tag{3.44}$$

where δV_j is the volume of the jth control volume, $x_{i,j}$ and $y_{i,j}$ are the liquid and vapour mass fractions, respectively, of the ith component in the jth control volume, $\rho_{V,j}$ and $\rho_{L,j}$ are the gas and liquid densities in the jth control volume and α_j is the void fraction in the jth control volume [49]. The local composition $C_{j,i}$ of the ith working fluid in each control volume is calculate as follows:

$$C_{j,i} = \frac{\delta M_{j,i}}{\delta M_j} \tag{3.45}$$

By combining Equation 3.43 and Equation 3.45, the local mass composition of the ith working fluid in each control volume is obtained as follows:

$$C_{j,i} = \frac{y_{i,j}\rho_{V,i}\alpha_i + x_{i,j}\rho_{L,i}(1-\alpha_i)}{\rho_{V,i}\alpha_i + \rho_{L,i}(1-\alpha_i)} \tag{3.46}$$

where the void fraction α is estimated using the Smith correlation [50]:

$$\alpha = \frac{1}{1 + (\frac{1-X}{X})\frac{\rho_V}{\rho_L}S} \tag{3.47}$$

where S is the slip ratio and it is computed:

$$S = K + (1-K)\left[\frac{\frac{\rho_V}{\rho_L} + K(\frac{1-X}{X})}{1 + K(\frac{1-X}{X})}\right]^{\frac{1}{2}} \tag{3.48}$$

where K is namely the ratio of the mass of liquid flowing in the homogeneous mixture to the total mass of water flowing, and it is recommended to be set to K = 0.4 [50]. The correlations proposed are based upon the following assumptions [50]:

1. The flow is stratified (annular) with a homogeneous mixture phase and a liquid-phase.
2. The homogeneous mixture of liquid and gas behaves as a single fluid with variable density (no separate momentum balances, no interfacial shear model).
3. Thermal equilibrium exists, i.e. the quantity of vapour present can be derived from a heat balance - at each control volume, liquid and vapour are at saturation, phase equilibrium compositions are valid, no subcooled boiling, no superheated vapour inside the two-phase zone.

When investigating the change in local composition $C_{j,i}$, as a function of vapour quality, Equation 3.46 can be re-arranged as it follows:

$$C_{j,i} = \frac{(1 - X_j)S_j x_{j,i} + X_j y_{j,i}}{(1 - X_j)S_j + X_j} \tag{3.49}$$

Zhao et al. [49] also defines the local composition in thermodynamic equilibrium as follows:

$$D_{j,i} = (1 - X_j)x_{j,i} + X_j y_{j,i} \tag{3.50}$$

These formulations can be used to quantify the local composition difference between composition and thermodynamic equilibrium, expressed as:

$$\delta = C_{j,i} - D_{j,i} \tag{3.51}$$

An iterative solution is then integrated to determine the change in composition based on the total and low-boiling point component hold-up mass. For each iteration, the hold-up mass in both evaporator and condenser are computed, summed up and used to define the circulating composition. Positive shift in composition will indicate the enrichment of the mixture of the more volatile component, while negative shift will symbolize a depletion in the latter. The model is built assuming uniform heat flux along the heat exchanger. As a consequence, each control volume receives the same amount of heat, and vapour quality varies linearly along the length of the heat exchanger.

4 Results

4.1 Characterization of in-situ determination methods

In this section the results of the prediction of the mixture properties as a function of changing composition are presented. The properties were estimated using REFPROP at constant evaporation pressure (P_{evap} = 3.20 bar) and condensation pressure (P_{cond} = 12.81 bar). For each pressure level, the temperature was fixed relative to the saturation condition by imposing a fixed temperature difference, either in the form of fixed degree of subcooling for the liquid phase properties, or fixed superheating for the vapour phase properties, depending on the chosen measurement location. It should be noted that the presented results are obtained from thermodynamic simulations and do not necessarily represent the actual phase state of the refrigerant mixture at a specific measurement point in the system. In particular, properties are evaluated for both liquid and vapour phases at each pressure level, even though only one of these phases may be physically representative at the given sensor location. This approach is intentionally adopted to isolate and analyse the sensitivity of the thermophysical properties to changes in mixture composition, independent of the local quality. By doing so, the analysis highlights the sensitivity of a given property also on whether the property is estimated in the liquid or vapour phase.

4.1.1 Density-based approach

Figure 4.1 and Figure 4.2 illustrate the change in density of the mixture as a function of the mixture composition. Here very different trends are observed based on whether the density is calculated in the liquid- or vapour-phase. The liquid density for both pressure levels (see Figure 4.1a and Figure 4.2a) exhibit non-monotonic behaviour with maximum values at intermediate to high concentrations of Isopentane. The exact location of the maximum is slightly shifted towards higher concentration of Isopentane for the lower pressure case (see Figure 4.1a). Nevertheless, the slope is quite significant around the charged composition.

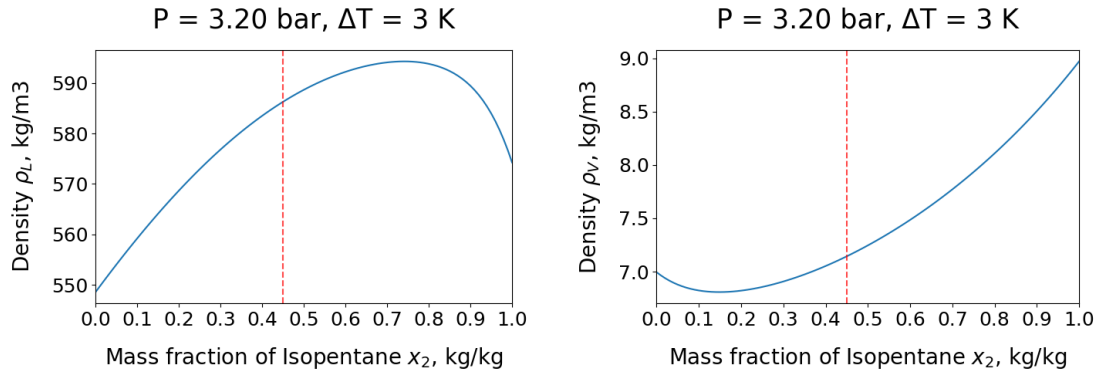

(a) Density in liquid phase.

(b) Density in vapour phase.

Figure 4.1: Liquid (a) and vapour (b) density curves as functions of mixture composition at constant pressure (P=3.20 bar) and fixed temperature difference (ΔT=3 K) from REFPROP.

From the perspective of using density as a property to determine the mixture composition, the bell-shaped curve implies that for a given measured liquid density value, two

different mixture compositions may satisfy the same density. Constraining the inverse problem, previously described, with the expected composition range in the proximity of the charged composition, can resolve the ambiguity of the results. The vapour density

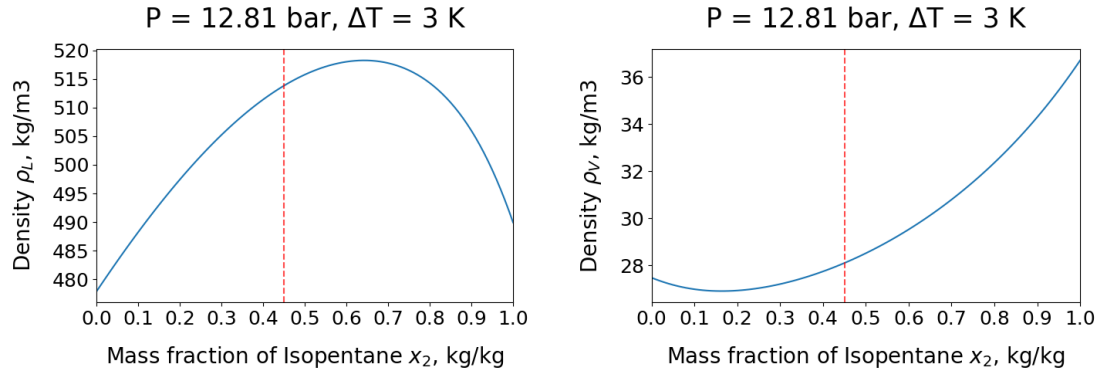

(a) Density in liquid phase.

(b) Density in vapour phase.

Figure 4.2: Liquid (a) and vapour (b) density curves as functions of mixture composition at constant pressure (P=12.81 bar) and fixed temperature difference (ΔT=3 K).

shows a more distinct trend with an increase in property with Isopentane fraction for both pressure levels. The monotonic behaviour thus ensure robust numerical inversion for composition determination.

4.1.2 Speed of sound-based approach

Figure 4.3 and Figure 4.4 depict the speed of sound of the mixture as a function of the mixture composition at the evaporator and condenser pressures, respectively. When comparing the steepness of the change in the property as a function of Isopentane mass fraction, it is observed that the speed of sound at the vapour phase (see Figure 4.3b and Figure 4.4b), has a higher sensitivity to the mixture composition, compared to the same property calculated in the liquid phase.

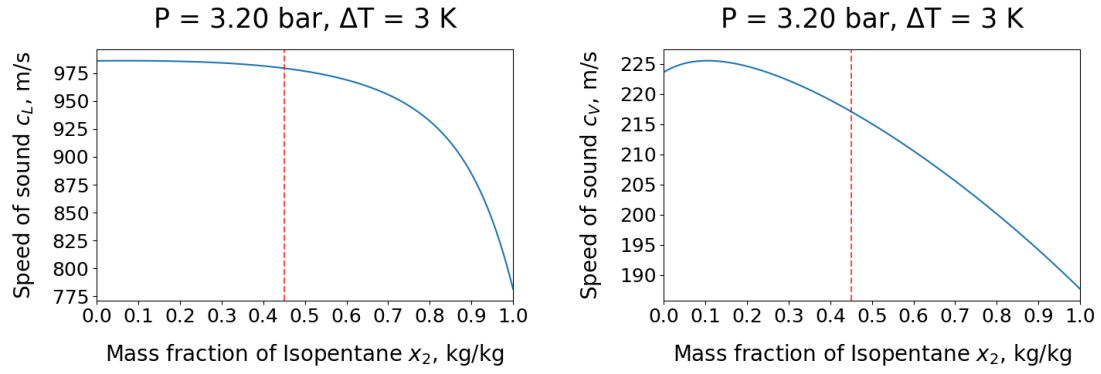

(a) Speed of sound in the liquid phase.

(b) Speed of sound in the vapour phase.

Figure 4.3: Liquid (a) and vapour (b) speed of sound curves as functions of mixture composition at constant pressure (P=3.20 bar) and fixed temperature difference (ΔT=3 K).

As a matter of fact, Figure 4.3a and Figure 4.4a show a smooth curve around the charged composition of the mixture (indicated by the red dashed line). The reduced slope at low

to medium Isopentane concentration, make the composition variation difficult to detect. On the other hand, the strong composition sensitivity, with a steeper slope especially at lower pressure (see Figure 4.3b), make the vapour phase speed of sound particularly suitable for in-situ measurements, especially near the evaporator or at the suction line of the compressor.

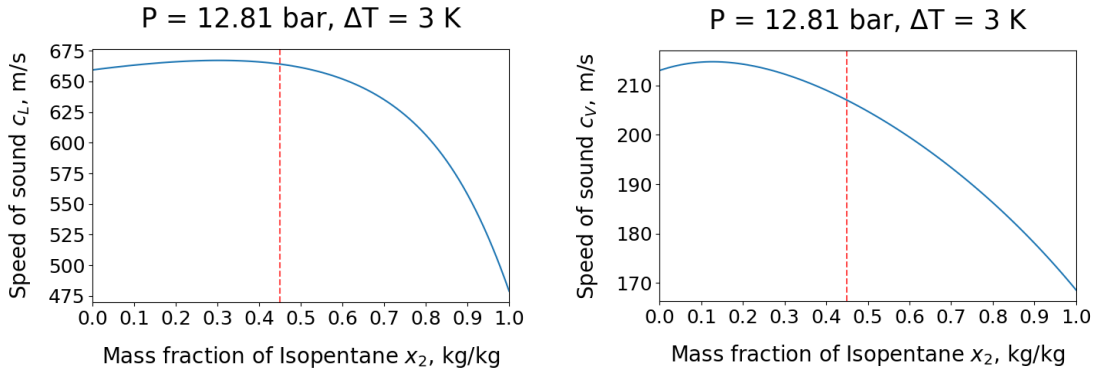

(a) Speed of sound in the liquid phase.

(b) Speed of sound in the vapour phase.

Figure 4.4: Liquid (a) and vapour (b) speed of sound curves as functions of mixture composition at constant pressure (P=12.81 bar) and fixed temperature difference (ΔT=3 K).

4.1.3 Enthalpy-based approach

The PTh in-situ composition determination method was applied by enforcing an isenthalpic constraint. The approach relies on measurements of pressure and temperature at two locations upstream and downstream of the throttling element and uses an equation-of-state-based property model to determine the mixture composition. For a trial composition, the specific enthalpy at both measurement locations is calculated using REFPROP as a function of the measured pressure, temperature, and mixture composition. The composition is then adjusted iteratively until the calculated upstream and downstream enthalpies match, thereby satisfying the isenthalpic constraint. The method is valid only when both upstream and downstream states remain single-phase, as the presence of two-phase flow would violate the assumptions of uniform thermodynamic state and introduce ambiguity in the enthalpy calculation. For this reason, compositions leading to two-phase conditions are excluded from the analysis.

4.1.4 Uncertainty propagation analysis

Considering that no experimental data was readily available for the Propane-Isopentane mixture, the analysis on uncertainty propagation was performed using the data present in the literature [4]. The PTD method was applied to the binary mixture R1224yd(Z)/R32 using measured pressure, temperature and density. A Monte Carlo uncertainty analysis was subsequently performed by perturbing the measured pressure, temperature, and density within sensor uncertainty bounds, reported in Table 3.2. The resulting distribution of the inferred composition yielded a standard deviation of $\pm$0.027 over the predicted composition, indicating a moderate sensitivity of the estimated composition to measurement noise. To further quantify the influence of individual measurement uncertainties, a linear error propagation analysis was conducted. The total propagated uncertainty of $\pm$0.026 was observed, in close agreement with the previous Monte Carlo analysis. Considering that the low-pressure piezolectric was employed, the analysis of the variables uncertainty showed that the temperature measurement was the biggest contributor to the total vari-

ance, contributing by approximately 88%. Pressure uncertainty resulted in around 11% and density contributed by 1%. The same analysis can be performed for the other methods given experimental data on speed of sound, temperature and pressure measurements at the upstream and downstream of the expansion valve.

4.2 Prediction of VLE behaviour of refrigerants-oil mixture

4.2.1 Model Formulation and Validation

In this section the results of the model predicting the VLE behaviour of the refrigerants-oil mixtures are presented, following the approach outlined in section 3.3. Three distinct approaches were adopted to find the binary interaction parameters for the three binary pairs. Each binary combination was treated independently using the formulations best suited to its physical behaviour and data availability. The resulting interaction parameters were then combined to build the three-components mixture model described in paragraph 3.3.2. First, the Propane-Isopentane pair was modelled using a VLE framework based on the PR EoS formulation. Secondly, the Propane-Oil pair was modelled fitting the available experimental data to the NRTL model, used to describe the non-ideality of the mixture. Finally, the Isopentane-oil mixture was simulated using an empirical correlation proposed as a first approximation of the mixture behaviour when no experimental data is available. Particular attention was given to the formulation of the last model, and a comparison with published data for a different mixture is presented in section A.2. Figure A.1 and Figure A.2 compare the pressure-oil concentration relations predicted by Fleming et al. [36] with the results of the present model. It is observed that for the two mixtures simulated, R22-SW46 and R134a-SW46, the model reproduced the overall trends plotted in the literature. At constant temperature, the equilibrium pressure decreases with increasing oil concentration, reflecting the suppression of the refrigerant vapour phase due to dilution in the oil-rich liquid phase [36]. Especially at low oil concentration, the model seems to realistically represent the reference literature results for all the operating temperatures plotted. However, as the oil concentration increases, increasing deviations between calculated and reference pressures are noticed, specially for higher temperature conditions. This behaviour is consistent with the findings reported by Fleming et al. [36], who noted that non-ideal effects become more pronounced at elevated temperatures and high oil concentrations, where uncertainties in activity coefficient models and binary interaction parameter correlations have a greater impact on the predicted equilibrium. Nevertheless, despite the deviations, the model seems to capture the behaviour of the mixture over the temperature and oil concentration ranges most relevant for the present study.

4.2.2 Prediction of VLE of binary mixtures

Figure 4.5 shows the solubility of Propane and Isopentane with the PAG 68 compressor oil. Specifically, Figure 4.5a illustrates the experimental data obtained from the literature [17], while Figure 4.5b depicts the behaviour of the oil-rich mixture with Isopentane, modelled using the molecular-weight-ratio NRTL-based model, described in subsection 3.3.4. The general trend observed is for the pressure of the refrigerant-oil mixture to increase as the oil concentration decreases (with increasing mass fraction of the refrigerant component) at constant temperature. The oil effectively dilutes the refrigerant in the liquid phase, so that only a small fraction of the dissolved refrigerant contributes to the vapour phase, leading to low equilibrium pressures at oil-rich conditions. An increase in system pressure is also noticed for increase in temperature for both mixtures.

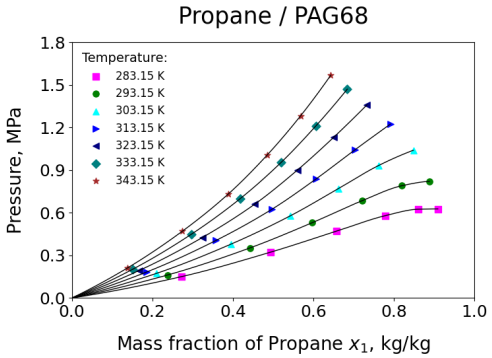

(a) Propane and PAG 68 oil.

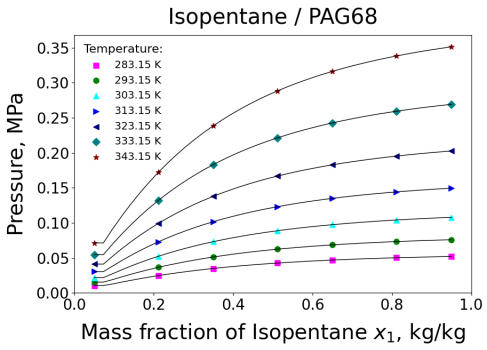

(b) Isopentane and PAG 68 oil

Figure 4.5: Solubility of Propane (a) and Isopentane (b) with PAG 68 oil at different temperatures.

Propane and Oil

In particular, Figure 4.5a exhibits the behaviour of the Propane-PAG 68 mixture as a function of increasing Propane concentration x_1. The bubble-point pressure curves for the different temperature levels appear to be quite steep, indicating a sharp pressure rise as the concentration of oil in the mixture decreases. Unlike Figure 4.5b, Figure 4.5a displays no curve flattening, especially at higher temperatures. On the contrary, temperature has an amplifying effect, with rapid increase in pressure even for low to moderate Propane concentrations at higher temperature conditions. These observations denote the high volatility and low solubility of Propane, which is thus weakly retained by the oil, and results in large increase in pressure even for small increments in Propane mass fractions.

Isopentane and Oil

Similarly, Figure 4.5b shows the behaviour of the Isopentane-PAG 68 mixture as a function of increasing Isopentane concentration. Figure 4.5b shows that at low Isopentane mass fractions, the pressure increases rapidly with composition, whereas at higher mass fractions, the curves gradually flatten, approaching the vapour pressure of nearly pure Isopentane. This behaviours suggests strong non-ideal mixing at oil-rich conditions and a diminishing marginal influence of additional refrigerant as the refrigerant concentration in the mixture increases. Looking at the different temperature conditions simulated, increasing the temperature translates the pressure curves upwards. In particular, temperature sensitivity is more pronounced at higher x_1, where the pressure is mainly governed by Isopentane volatility. At lower x_1, pressure remains low even for higher temperatures, reflecting the strong retention of the refrigerant in the oil-rich liquid phase. Overall, the moderate volatility and good solubility of Isopentane in PAG 68 oil results in low vapour-phase fugacity and moderate suppression of pressure for low Isopentane concentration, while pressure approaches pure-component behaviour for higher Isopentane concentrations.

Propane and Isopentane

Figure 4.6a shows the mixture pressure as a function of Propane mass fraction, for the Propane-Isopentane binary mixture for T = 323.15 K (at suction line of the compressor). The curve shows a smooth increase in equilibrium pressure with increasing Propane concentration, reflecting the higher volatility of Propane compared to Isopentane. This behaviour is consistent with the large difference in normal boiling points and critical pressures of the two components. As Propane content increases, the vapour phase becomes increasingly dominated by Propane, leading to a rapid increase in saturation pressure

even for modest changes in composition. At intermediate compositions, the curves exhibit a pronounced non-linearity, indicating non-ideal VLE behaviour. This is in good agreements with the trends observed in Figure 3.2, displaying the data reported by Vaughan & Collins [13]. Figure 4.6b also shows the progressive separation of the curves at higher temperatures, reflecting the temperature dependence of vapour pressure and the non-ideality of the mixture. The strong sensitivity of pressure to composition on the Propane-rich side also implies that small composition shifts during phase change can lead to significant pressure variations.

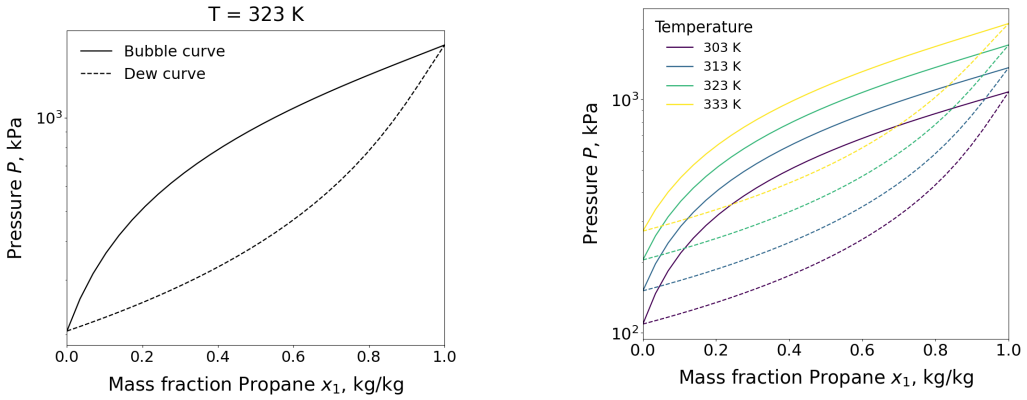

(a) Curve for T = 323.15 K.

(b) Effects of temperature on pressure.

Figure 4.6: Bubble- and dew-point pressure curves of the Propane–Isopentane mixture as a function of Propane mass fraction.

Propane, Isopentane and Oil

In conclusion, the three components mixture, comprising of Propane, Isopentane and PAG 68 oil was modelled and the results are shown in Figure 4.7, where the equilibrium pressure is plotted as a function of the total refrigerant mass fraction in the liquid phase. Consistently with the behaviour of the binary mixtures Propane-Oil and Isopentane-Oil viewed in Figure 4.5, the ternary mixture depicted in Figure 4.7, exhibits a steep pressure rise at low refrigerants mass fraction, and a smoother increase for higher refrigerants mass fractions. The liquid phase is dominated by oil at low refrigerants concentrations, and the refrigerants fugacity is thus strongly suppressed, and consequently, small additions in refrigerants content leads to sharp increases in pressure. As the total mass of refrigerants increases, the curves gradually flatten as the pressure becomes increasingly governed by the volatility of the Propane-Isopentane blend, rather than oil interactions. Generally, Propane, being more volatile, dominates the pressure response at higher refrigerant fractions, while Isopentane moderates the pressure rise through stronger solubility in the oil phase.

4.2.3 Prediction of VLE of ternary mixtures

For the mixture Propane (1), Isopentane (2) and PAG 68 oil (3), the following binary interaction parameters ($\Delta\lambda_{ij}$) were found:

$$\Delta\lambda_{12} = 1191.7 \qquad \Delta\lambda_{13} = 7799.25 \qquad \Delta\lambda_{23} = 2695.8$$
$$\Delta\lambda_{21} = -846.75 \qquad \Delta\lambda_{31} = -1999.92 \qquad \Delta\lambda_{32} = -3132.1$$

In the NRTL framework, $\Delta\lambda_{ij}$ represent the difference in interaction energy between unlike and like molecular pairs. The higher the value of the interaction parameters, the

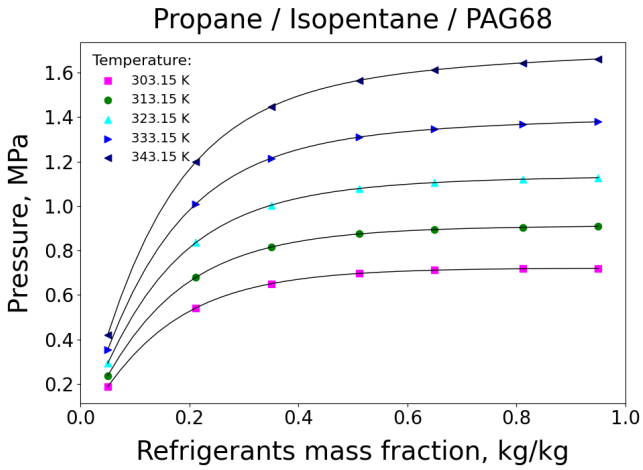

Figure 4.7: Solubilities of Propane-Isopentane with PAG 68 at different temperatures.

stronger the non-ideality of the binary mixture. Moreover, positive values of $\Delta\lambda_{ij}$ indicate energetically unfavourable $i-j$ interactions, while negative values of $\Delta\lambda_{ij}$ reveal energetically favourable $i-j$ interactions [51]. The asymmetry in values for a binary pair (i.e $\Delta\lambda_{ij} \neq \Delta\lambda_{ji}$) thus reflects the differences in molecular size, polarity and specific interactions between the components' molecules [28]. The modelling of the pair Propane-Isopentane resulted in the binary parameters $\Delta\lambda_{12}$ = 1191.7 and $\Delta\lambda_{21}$ = -846.75. The relative small numbers hint to moderate non-ideality between Propane and Isopentane. This is consistent with the rather small binary interaction parameter k_{ij} obtained from the study of Seif Eddeen at al. [33], which also implies weak to moderate non-ideality of the mixture. The results additionally agree with the similarity in chemical nature of the two components, being both non-polar hydrocarbons but with different molecular sizes and volatilities. On the contrary, considerably different interaction parameters are found for the pair Propane-Oil, with $\Delta\lambda_{13}$ = 7799.25 and $\Delta\lambda_{31}$ = -1999.92. The large positive $\Delta\lambda_{13}$ suggests a strong energetic mismatch between Propane and PAG 68 molecules, resulting in unfavourable Propane-Oil interactions. This reflects the large molecular size discrepancy, the strong polarity difference and thus weak affinity between the two mixture components' molecules. Contrarily, the negative $\Delta\lambda_{31}$ reveals that from the oil's molecules perspective, Propane is slightly stabilizing. In general, the calculated parameters prove the poor solubility of Propane with the PAG 68 oil, which can potentially affect the equilibrium pressure of the binary mixture. Finally, the modelling of the Isopentane-Oil mixture provided the interaction parameters $\Delta\lambda_{23}$ = 2625.8 and $\Delta\lambda_{32}$ = -3132.1. It is noted that the magnitude of $\Delta\lambda_{23}$ is substantially smaller than that of $\Delta\lambda_{13}$. It follows that Isopentane molecules will tend to interact more favourably with the oil molecules, than Propane. This also agrees with the higher solubility of Isopentane with PAG 68 oil. Conversely, the highly negative value for $\Delta\lambda_{32}$ suggests a stabilizing effect of Isopentane on the oil molecular structure, consistent with the larger molecular size, and higher polarity. The three pairs of interaction parameters were then used as inputs for the ternary mixture model, described by Equation 3.31 to quantify the combined effects of preferential solubility of Propane and Isopentane with the oil. The calculation was performed at a temperature of 323.15 K and a system pressure of 3.2 bar. The charged composition of the blend was set to 55% Propane and % Isopentane, to which a lubricant mass fraction of 10% was added. The

resulting overall mass fraction vector was therefore:

$$z_{\text{charge}} = [0.495,\ 0.405,\ 0.10]$$

Flash calculation at these conditions showed a reduction in vapour fraction to 0.953, indicating dominance of the vapour phase, with the presence of small mass in the liquid phase, strongly enriched in oil. The predicted compositions in the vapour- and liquid-phase were the following:

$$y_{\text{circ}} = [0.5679,\ 0.4321]$$

$$x_{\text{circ}} = [0.0348,\ 0.2338,\ 0.7314]$$

The vapour composition of the mixture estimated by the model showed an enrichment in Propane relative to the charged composition. The result reflects the higher volatility and lower molecular weight of propane compared to Isopentane, which causes Propane to preferentially partition into the vapour phase at equilibrium. Since the oil is non-volatile, it does not appear in the vapour phase. On the other hand, the blend composition in the liquid phase showed big percentage of oil, with more than 73% of the total mass consisting of only lubricant. Considering the refrigerants fraction of the total mass, Isopentane dominates the liquid phase, while Propane was heavily depleted. This behaviour confirmed the preferential solubility of Isopentane in the oil, a consequence of its higher molecular weight, lower volatility, and stronger affinity for the lubricant phase. To quantify the net effect of oil-induced phase separation on the refrigerant mixture, the effective refrigerant composition was computed by mass-weighting the vapour and liquid refrigerant compositions according to the vapour fraction using Equation 3.35, resulting in an overall enrichment in Propane as it follows:

$$z_{\text{circ}} = [0.5622,\ 0.4378]$$

4.2.4 Temperature rise

Figure 4.8 shows the shift in saturation temperature as a function of increasing oil concentration. Figure 4.8a shows the results of the empirical correlations described in Equation 3.39, while Figure 4.8b illustrates the results of the present thermodynamic model explained in subsubsection 3.3.6. Overall, both approaches demonstrate a similar trend. The presence of oil leads to an increase in bubble-point temperature of the mixture at constant pressure, due to the reduction of effective refrigerant fraction of in the liquid phase due to increase oil retention. At low oil concentrations, both models predict a minor temperature rise. In this region, the refrigerants remain the dominant component in the liquid phase, and deviations from ideality are limited, and associated mainly to non-ideality of the Propane-Isopentane pair, leaving the oil to have minimal effects on the saturation properties of the mixture. This is consistent with practical heat pump systems where circulating oil concentrations are typically low and oil effects on saturation properties are minimal and neglected [5]. Nevertheless, for higher oil concentration, strong non-linear behaviour emerges in both the curves, with rapid increase in temperature for $w_{\text{oil}} > 0.5$. This can be explained by the fact that the refrigerants in the mixture gets increasingly dissolved in the oil-rich liquid phase, and progressively higher temperatures are required to generate sufficient refrigerant vapour pressure to satisfy equilibrium at constant pressure.

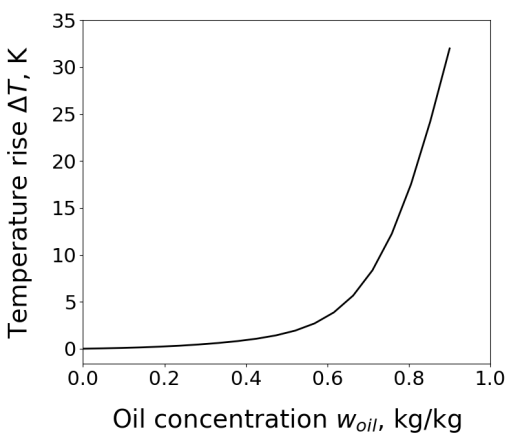

(a) Literature model [36].

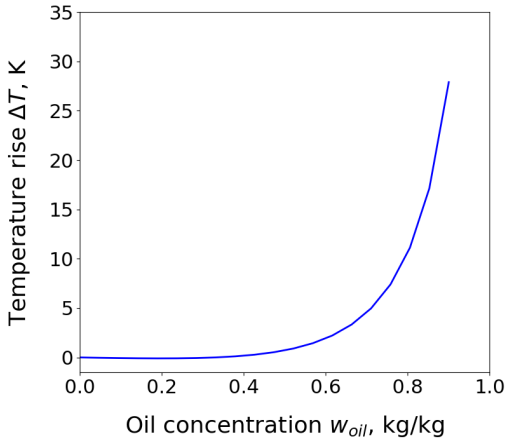

(b) Present model.

Figure 4.8: Temperature rise of Propane-Isopentane-Oil resulting from the (a) reference model and (b) present model.

Despite the similar trend, Figure 4.8a predicts higher temperature rise for high oil mass concentrations compared to Figure 4.8b. The discrepancy in results may be attributed to the fact that the empirical model does not account for components-dependent activity coefficients, but rather on empirical constants. The simplified dependence of temperature on the oil concentration, independent on the oil type and solubility with the other elements in the mixture, may not fully be representative of the actual thermodynamic behaviour of the ternary mixture, while still showing good agreement with the overall trend. Moreover, the higher oil concentrations where the differences are more significant, are out of the range of expected concentration of oil in the circuit, and do not meaningfully impact the validity of the models.

4.3 Local composition modelling

This section presents the results of the model developed to predict the local composition shift for the binary mixture Propane-Isopentane, following the mass-based framework described by Zhao & Bao [49] and introduced in details in section 3.4.

4.3.1 Numerical model development and validation

The primary objective of the model is to provide information on the distribution of the two components in the two-phase region of the evaporator and condenser and determine the resulting deviation from the charge composition under steady-state operations. It is important to note that the presence of the lubricating oil in the heat exchangers was neglected. This is consistent with the methodology proposed by the literature that aims at isolating and quantifying composition shift arising exclusively from two-phase mass hold-up and vapour-liquid slip effects. To estimate the circulating composition of the two components in the mixture, a linear enthalpy distribution between bubble and dew points was assumed, hence implying uniform distribution of heat rejection and absorption mechanisms per unit length of the heat exchangers. This simplification decouples the composition-shift calculation from uncertainties associated with two-phase heat-transfer correlations, which have not been investigated in this study. The validity of this assumption was discovered to be strongly dependent on the spatial resolution of the model. For this reason, an analysis on the number of discretized control volumes was required to ensure that the imposed linear enthalpy profile was resolved without showing abrupt changes in vapour quality, phase densities and void fraction. By progressively increasing the number of control volumes, the enthalpy change across each element was reduced, and the thermodynamic state within each control volume approached a locally linear behaviour. Discretizing the heat exchangers' length by 500 elements, allowed the aforementioned properties to vary smoothly along the heat exchanger length and guarantee that the difference between local circulating composition at the inlet and outlet of each heat exchanger was minimized.

4.3.2 Local composition of working fluids during phase change

The developed control volume-based mixture model (described in section 3.4) was used to analyse the local composition and mass hold-up behaviour of the Propane-Isopentane mixture. As also mentioned before, the effects of the oil was neglected and the working fluid was treated as a binary refrigerant mixture. However, the effects of oil may be considered to be implicitly accounted for since the input composition of Propane–Isopentane mixture used in the analysis (named as "charge composition" in the model) corresponds to the effective refrigerant composition (z_{eff}) obtained from the preceding oil–refrigerant equilibrium study, which quantified the amount of Propane and Isopentane retained in the oil-rich liquid phase. Figure 4.9 shows the change in local composition over the discretized length of the heat exchangers, here expressed as a function of the mixture vapour quality. Specifically, Figure 4.9a shows the liquid phase composition in the two-phase zone of the evaporator. It can be observed that the local composition of Propane and Isopentane are initially close to the charge composition, and they increasingly deviate with increasing quality. Propane concentration reaches a minimum around quality X=0.7-0.8 and it recovers towards the evaporator outlet. On the contrary, Isopentane concentration shows an opposite trend, increasing above the charge composition and peaking at the same quality range where Propane reaches a minimum. Its concentration then slowly decreases closer to the evaporator outlet. Overall, Figure 4.9a preferential evaporation of the two components in the mixture occurs because of the differences in volatility and boiling points. Propane, which is more volatile, as evaporation proceeds, will preferentially enter the vapour phase, thus getting depleted in the liquid phase illustrated in Figure 4.9a. Generally, compared to the charge composition, the local mass fraction of the low-boiling

point Propane has negative variation with vapour quality, while that of the high-boiling point Isopentane has positive variation.

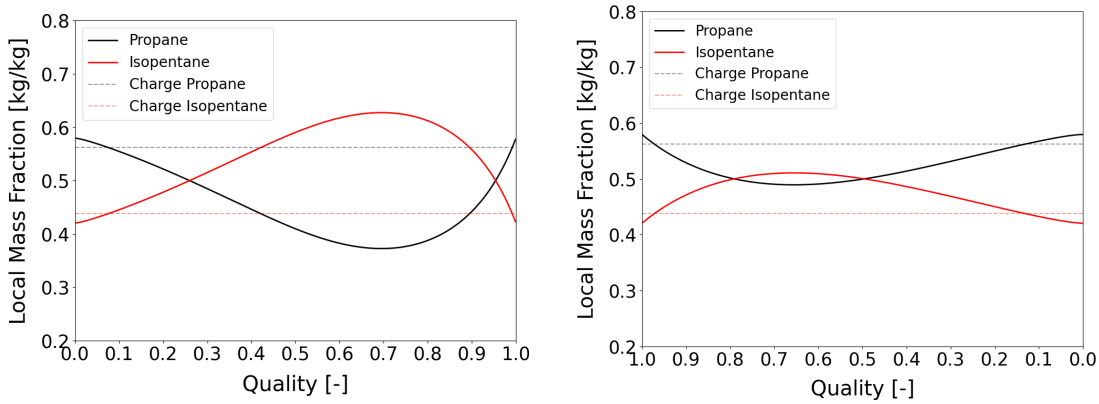

(a) evaporator model

(b) Condenser model.

Figure 4.9: Variation of the local mass fraction for the working fluids in the evaporator (a) and condenser (b) as a function of vapour quality.

Similarly, Figure 4.9b shows the change in local composition of Propane and Isopentane in the condenser. At the inlet of the condenser, for X = 1.0, the mixture is saturated vapour, enriched in the more volatile component Propane. As condensation begins, Propane condenses preferentially because of its high saturation pressure and low-boiling temperature, hence the first liquid formed is rich in Propane. The remaining vapour is accordingly enriched in Isopentane. However, due to slip ratio effects, liquid moves slower than the vapour phase and it will accumulate locally. This results in the Propane mass fraction to decrease while the one of Isopentane increases. Figure 4.10 and Figure 4.9b illustrate the composition variation of Propane and Isopentane in the gas, liquid and total two-phase flow, as a function of the vapour quality. The behaviour is consistent with the behaviour previously observed in Figure 4.9. In both Figure 4.10a and Figure 4.11a, Propane concentration of the gas phase is always greater than that of liquid. The gas phase is thus always Propane-rich over the entire two-phase region in the evaporator. This is confirmed also by the continuous decrease in concentration of the Propane liquid-phase as the evaporation proceeds. Overall, local Propane concentration demonstrate negative variation as the most volatile component in the mixture. On the other hand, the Isopentane concentration in the gas phase is always lower than the one in the liquid phase. This also aligns with previous observations on the difference in volatilities between the two components. As the vapour quality increases, Propane preferentially evaporates into the gas phase, while Isopentane remains in the liquid phase. The liquid phase mass fraction of Isopentane will thus increase, as in Figure 4.10b, while the gas phase gets increasingly depleted by Isopentane and dominated by the more volatile Propane. Hence, Isopentane local concentration will have positive variation.

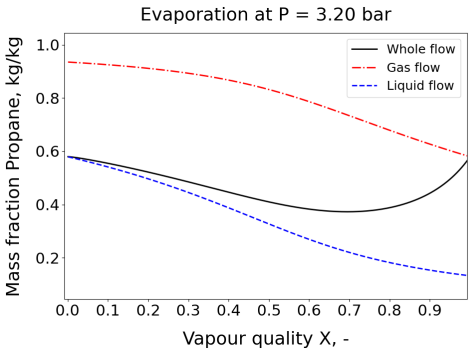

(a) Propane.

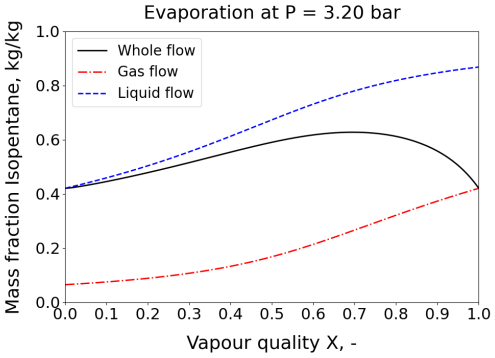

(b) Isopentane.

Figure 4.10: Local mass concentration of Propane (a) and Isopentane (b) along the evaporator length.

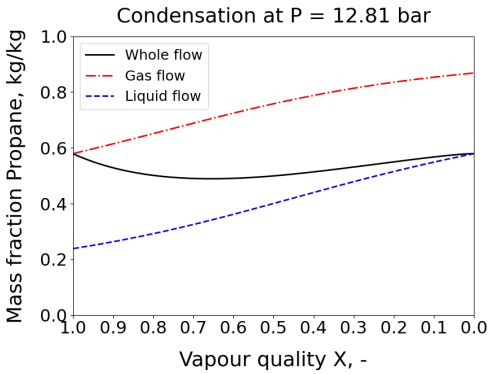

(a) Propane.

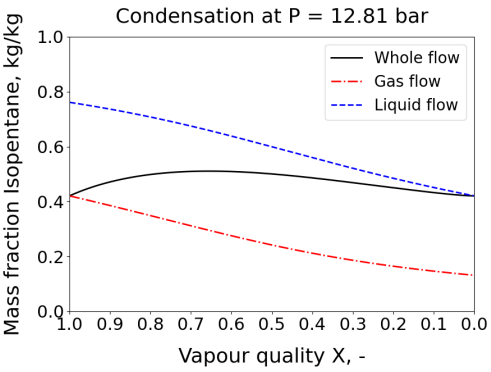

(b) Isopentane.

Figure 4.11: Local mass concentration of Propane (a) and Isopentane (b) along the condenser length.

From a quantitative perspective, the model predicts a deviation of composition from the initial 56.22% Propane/43.78% Isopentane to 57.9% Propane/42.1% Isopentane, corresponding to a relative enrichment of Propane by +3.1% and equivalent depletion of Isopentane by -3.1%. These results agree with the aforementioned observations which showed that considering that the circulating mass flow is dominated by vapour transport, the circulating mixture becomes enriched in Propane relative to the original charge. An additional important result of the analysis is the magnitude of the refrigerant hold-up in the evaporator and condenser calculated using Equation 3.44. Of the total charged mass assumed to be 0.35 kg, approximately 0.136 kg is retained as hold-up within the heat exchangers, corresponding to nearly 39% of the total charge. It follows that only about 0.214 kg actively participates in circulation. Finally, the deviation between the local composition and its equilibrium value (as defined by Equation 3.51) was evaluated as a direct indicator of phase slip and density differences that drive the mixture away from equilibrium. The maximum values for such difference demonstrated that the deviation is most pronounced in the evaporator (δ_{evap} = 0.207) compared to the one recorded in the condenser (δ_{cond} = 0.09) in absolute values.

4.3.3 The effect of charge on circulating composition

Supplementary study on the variation of circulating composition as a function of charge was carried out using Equation 3.42, which can be further derived [52]:

$$z_{\text{cir}} = \frac{z_j M_{\text{charge}} - \sum M_{\text{j,hold-up}}}{M_{\text{charge}} - \sum M_{\text{hold-up}}} = z_j + \frac{\sum (z_j - C_{j,i}) z_{\text{hold-up}}}{M_{\text{charge}} - \sum M_{\text{hold-up}}} \tag{4.1}$$

It is noted from Equation 4.1 that when the charge mass is small, the two-phase liquid hold-up mass becomes a large fraction of the total mass, thus resulting in significant local composition effects. Contrarily, as the the total charge mass increases, there will be a decrease in circulating composition of the low boiling point component. The results are also visually displayed in Figure 4.12, where the total charge mass of the mixture is plotted against the circulating mass fraction of the low boiling point refrigerant (Propane) and the one of the high boiling point refrigerant (Isopentane). It is observed that when the charge increases, the same hold-up mass becomes less important, and the circulating composition approaches the charged composition asymptotically, creating a steep slope at low charge and flatten curve at higher charge. The analysis followed with the conclusion that increasing the charge mass can mitigate the effect of composition shift. Nevertheless, increasing the charge can result in increase in system investment costs, and increasing the charge for removing the influence of composition shift is considered not optimal by the literature [49, 52].

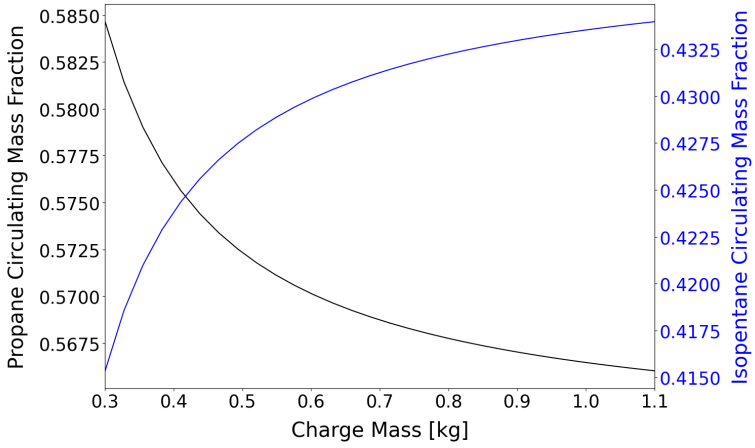

Figure 4.12: The effect of charge on the circulating composition.

4.3.4 Effect of composition shift on heat pump performance

Table 4.1 summarizes the results of the change in composition obtained from dual analysis on preferential oil solubility and liquid hold-up. Starting from a charged composition of 55/45 (Propane-Isopentane by mass), the effective composition obtained after accounting for oil–refrigerant equilibrium shows a slight enrichment in Propane (56.2%). When two-phase flow and mass hold-up are further considered, the circulating composition shifts even further, turning into 57.9% Propane and 42.1% Isopentane. In general, the net composition shift relative to the charged mixture equals to +3.06% increase in the mass fraction of Propane and matching decrease in Isopentane, confirming the cumulative impact of the redistribution of the oil-induced and flow-induced composition.

Table 4.1: Calculated concentrations of the mixture components.

Concentration [kg/kg]	Propane	Isopentane
Charged (z_{charge})	0.55	0.45
Effective (z_{eff})	0.562	0.438
Circulating (z_{circ})	0.579	0.421
$z_{shift} = z_{charge} - z_{circ}$	+3.06%	-3.06%

Figure 4.13 visually illustrates the relationship between charged propane mass fraction and the resulting circulating mass fractions of Propane and Isopentane. Beyond illustrating the sensitivity of the circulating composition to the charged mixture, this relationship can be used as a practical design tool. In particular, the figure enables the prediction of the required charge composition needed to achieve a desired circulating composition. This is especially relevant when the optimal mixture composition is identified through a prior screening or optimisation process aimed at maximising cycle performance. By accounting for composition shift effects, the charged composition can be adjusted such that the circulating composition matches the target, performance-optimal mixture during operation, rather than merely at the point of charging.

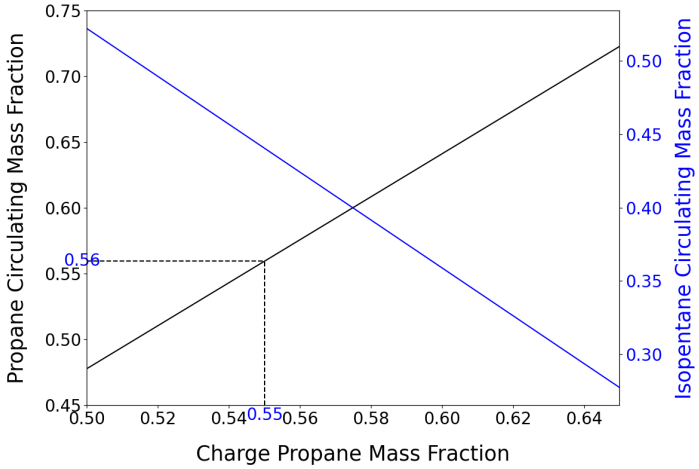

Figure 4.13: The effect of charge composition on the circulating composition.

Table 4.2 reports the effects of combined composition shift on the thermodynamic performance of a single-stage heat pump cycle with internal heat exchanger. The simulations were carried out for fixed source (40/7 °C) and sink (50/80 °C) temperature levels, ensuring that any variation in performance can be attributed solely to changes in blend composition rather than external operating conditions. Both the evaporating pressure and the condensing pressure rise as the mixture becomes progressively richer in Propane, reflecting the higher volatility of Propane compared to Isopentane. The increase is small but consistent, with a total pressure rise of 4.6% for both the evaporator and condenser conditions. However, despite the deviations in pressure levels, the net composition shift only slightly affects the performance of the cycle for the given operating conditions. As a matter of fact, the COP of the system decreases from 4.34 for charged composition to 4.31 for circulating composition. This demonstrates the relative insensitivity of the cycle efficiency to the moderate composition observed. Lastly, the volumetric heating capacity (VHC), shows a little increasing trend with Propane enrichment. The VHC rises from

2777 kJ/m^3 for the charged composition to 2885 kJ/m^3 for the circulating composition. This increase is consistent with the higher vapour pressure and density associated with Propane-rich mixtures and suggests a potential benefit in terms of compressor sizing and heating capacity, albeit at the expense of slightly higher operating pressures.

Table 4.2: Calculated performance changes caused by concentration shift.

Concentration	COP [-]	p_{evap} [bar]	p_{cond} [bar]	VHC [kJ/m^3]
z_{charge}	4.34	3.23	12.89	2777.0
z_{eff}	4.33	3.29	13.13	2822.0
z_{circ}	4.31	3.38	13.48	2884.6
z_{shift} [%]	-0.69	+4.64	+4.57	+3.87

5 Discussion

This chapter provides a critical discussion of the results, emphasising on the limitations and validity of the formulated thermodynamic models while also contextualizing the results obtained with the results presented in the literature.

5.1 In-situ measurements and sensors accuracy

As observed in the analysis of propagation of uncertainty, the precision and placement of sensors introduce uncertainty into the determination of mixture composition. Especially regarding the sensor precision, uncertainties from pressure and temperature measurements, which are not taken directly at the density and speed of sound sensors, inevitably introduce errors. Moreover, the analysis of the different methods for accessing experimentally the circulating composition of the mixture, showed the non-monotonic behaviour of the liquid density-based approach. A single measured density could satisfy simultaneously two different mixture compositions, requiring the numerical inversion to be constrained by an expected composition range to be measured. Lastly, the speed of sound measurements in the liquid phase exhibited reduced slope around the charged composition of the blend, making minor deviations in composition difficult to detect. In addition, without any direct measurements of oil, it is difficult to determine whether a change in measured property is due to a change in the refrigerants ratio or due to presence of oil in the system. In particular the speed of sound is strongly correlated with the amount of oil present in the liquid phase. According to the Gibbs phase rule, a single-phase binary mixture requires three independent intensive properties (such as pressure, temperature, and a third property like density or speed of sound) to uniquely define its state. To resolve a system with an extra component, like in the case of the oil-rich mixtures, a supplementary independent measurement should be incorporated. By comparing measurements from both a density sensor and an speed of sound sensor, the different sensitivity levels could possibly allow to differentiate whether a property shift is likely due to the refrigerant ratio (which affects both density and speed of sound) or oil presence (which primarily affects speed of sound).

5.2 Validation and prediction of phase behaviour in refrigerants-oil mixtures

A primary limitation to the modelling of the mixture is the lack of experimental data, which results in the need of using approximations or data generated using thermodynamic software. For the Isopentane-PAG 68 mixture, no experimental data was available. Hence, the study had to rely on an empirical correlation based on the molecular weight ratio of the oil to the refrigerant as a ”first approximation”. Moreover, no previous studies have investigated any of the blends examined in the present model (except for Propane-PAG 68), thus no validation of the actual binary coefficients was possible. The accuracy of these parameters is essential to confidently predict the behaviour of the mixture, as they strongly influence the composition shift of the blend in the system. Also, different thermodynamic mixture models are available, and a comparison between different models could be interesting to assess the impact of the model type on evaluating composition shift. In terms of accuracy, it is also important to note that manufacturer data for the compressor lubricant is available only for standard conditions, requiring the use of empirical correlations to estimate properties at operational conditions. Ultimately, the assumption of a

fixed 10% oil concentration without actual measurement represents a significant limitation in the study, as the circulating oil concentration directly dictates the magnitude of the composition shift associated with the retention of the refrigerants in the oil-rich liquid phase. At the initialized oil concentration, the model predicts an effective refrigerant composition of 56.22% Propane and 43.78% Isopentane. Because Isopentane is more soluble in oil than Propane, any change in the actual oil concentration would alter this ratio. If the real oil concentration were lower than 10%, the shift toward Propane-enrichment would be less pronounced; if higher, the shift would increase. Furthermore, the analysis of the dependency of pressure and bubble-point temperature on the oil concentration in the mixture, indicted that the sensitivity of the two properties increases as the oil fraction increases. Finally, preferential oil solubility is simulated only for one point in the system. However, considering that Isopentane is soluble in the oil phase, in the case of oil presence in other parts of the system, Isopentane retention in the oil-rich liquid phase would increase, thus further pronouncing the composition shift, in different parts of the circuit.

Temperature rise
The predicted influence of oil on the VLE properties of the refrigerant mixture in the present work is consistent with trends reported in previous studies. Fleming et al. [36] analyzed the temperature rise of the R134a/SW46 mixture, and demonstrated that the mixture follows closely the bubble-point temperature of pure R134a at oil concentrations lower than 60-70 wt%. In the same way, Burton et al. [35] detected a similar trend. In their study, the authors notices that the lubricant does not significant affect saturation mixture pressure and temperature until the refrigerant mass fraction is reduced to about 38%. A substantial effect is seen for refrigerant mass of 14%.

5.3 Local composition modelling

The primary limitation of the analysis on the local composition of the mixture during phase change is probably the disregard of the effects of lubricating oil. This is an intentional simplification designed to isolate and quantify the composition shift arising exclusively from two-phase mass hold-up and vapour-liquid slip effects. Nevertheless, some previous studies investigating the effects of oil on a vapour compression refrigeration (VCR) system, declared that the evaporator may be adversely affected by the oil lubricant presence in the system. In particular, the refrigerant-oil mixture can form an oil film at the evaporator surface due to the evaporation of the refrigerant liquid [53]. The oil film and vapour quality change due to oil local concentration adversely affect the dynamics of flow and the heat exchange in the evaporator, with a potential reduction by 4% of the cooling capacity of the system [54]. Secondly, the model assumed linear vapour quality, which decouples heat transfer calculations from uncertainties associated with two-phase heat transfer coefficient correlations for mixtures. Uniform heat flux is assumed along the two heat exchangers simulated, implying linear enthalpy distribution between bubble- and dew-points. Nonetheless, by increasing the number of control volumes that divide the heat exchangers into elements, convergence for the circulating composition at the inlet and outlet, was achieved. Also, as shown in Figure 3.6, only two-phase regions are assumed to contribute to hold-up and composition shifts, while single-phase regions are assumed to have constant composition. As shown Table 4.1 and Table 4.2, the change in circulating composition was found to be quite small in relation to the charged composition, and no significant effects were observed on the overall performance of the heat pump cycle simulated. However, the assessment does not include a dedicated analysis of the heat transfer phenomena specific to zeotropic mixtures, especially during phase change. Figure 4.9a and Figure 4.9b, showed significant redistribution of the mixture components in the heat exchangers, which adds on the uncertainty of the heat transfer performance,

demonstrated in previous studies to be potentially reduced when working with zeotropic mixtures. As a matter of fact, compared to pure fluids with constant composition during phase change, zeotropic mixtures exhibit additional heat transfer resistance emerging from their non-isothermal condensation, which entails continuous sensible cooling of both the condensate and the remaining vapour [19]. Plus, due to the concentration gradient observed, mass diffusion of the more volatile component occurs towards the bulk and of the less volatile component towards the interface [19]. Consequently, the extra heat and mass transfer resistances result in a degradation of the condensation rate, which causes the heat transfer coefficient of the mixture at a given composition to be lower than the weighted average of the corresponding pure component values [19]. Zhou et al. [52] explored the influence of local composition shift on heat transfer mechanisms, specifically on the temperature variation along the heat exchangers. In particular, the study reveals that in the evaporator the average temperature difference is smaller when accounting for local composition shift, which results in the need of larger heat transfer area [52]. Whereas, in the condenser the opposite phenomenon is discovered with lower average temperature difference and less heat transfer area needed. Nonetheless, the authors mention that temperature variation observed in zeotropic mixtures is still a novel subject and requires further research, and requires experimental verification, which is fundamental for correctly define effective heat exchangers. In light of this, the overall trends observed for composition shift in the two-phase region seems to agree with the results of similar studies presented in the literature. Youbi-Idrissi et al., [48] performed a comparable research for the R407c mixture (R134a/R125/R32). When modelling local composition, the authors observed the two composition shift peaks; the first peak happening at the beginning of condensation where less volatile component (R134a) condenses preferentially to the others. This is additionally supported by vapour velocity being higher than that of the liquid, specially at the beginning of condensation [48]. This peak is also distinguished in Figure 4.9b, where the largest difference between charged and circulating composition is recorded for high to intermediate qualities.The second peak, of larger magnitude, is then observed close to the evaporator end, because of the accumulation of R134a, which evaporates to a lower extent compared to the other more volatile component [48]. The work of Zhao et al. [49] demonstrated the same behaviour along the evaporator and condenser for the mixture Isobutane-Pentane, with the gas phase containing more Isobutane, whilst the liquid phase was depleted in the high boiling point component Pentane. Xu et al. [46] also differentiated between composition shift because of the inhomogeneous distribution of the refrigerants in a mixture, and composition shift existing in the gas-liquid flow with heat transfer. By underlining the difficulty in measuring local composition variation experimentally, the authors propose an energy and mass conservation based approach that allows to demonstrate the deviation of the local composition within a two-phase control volume from the nominal composition of the mixture. For the ternary mixture investigated, comprising of Methane (33%), Propane (33%), and Butane (34%), the study indicates negative variation of the most volatile component Methane, positive variation for Butane along the evaporator length. For the case of Propane, a certain point along the flow path is defined so that upstream the point, Propane concentration in the gas phase is lower than that in the liquid phase, leading to positive variation, whereas downstream the same point, the concentration in the gas phase exceeds that in the liquid phase, resulting in negative composition shift. Despite the higher complexity of the behaviour of Propane in the ternary mixture studied by Xu et al. [46], the trends and relations between composition shift and volatility are confirmed with the results of the present study.

5.4 Net Composition Shift

The thermodynamic model results showed a moderate cumulative composition shift, combining the solubility driven and slip induced effects, of approximately 3% difference with the charged composition. Zhang et al. [19] measured the deviation between charged and circulating composition experimentally, using the liquid density and enthalpy methods. The authors state good agreements of the two methods, with deviations in composition from the charge in the ranges from 0.5% to 2.9%, which also agree with the range observed with the Propane-Isopentane mixture. Youbi-Idrissi et al. [48] simulated the behaviour of the refrigerant R407 in a water-to-water heat pumps and noticed a reduction in circulating composition, in comparison to the nominal one, of the less volatile component R134a by around 3% (absolute deviation) and an enrichment by the same 3% of the more volatile component R32. R125 circulating mass composition remained quasi-constant. Zhao et al. [49] researched the influence of composition shift on an organic Rankine cycle with zeotropic mixtures. The authors discuss the local composition shift characteristic in the process of phase change, and discovered that the mass fraction (35.30%) of the low boiling point Isobutane in the circulating composition condition was +3.74% higher than that (31.56%) if the charge composition condition. This was explained mainly due to the difference in the speed of the working fluid between the gas and liquid phase and the different boiling points of the two components of the mixture in the phase change process [49, 48]. Despite this overall consistency, the present analysis is limited to a single set of operating conditions. Since composition shift is inherently sensitive to the operational conditions, additional simulations over a broader range of conditions would be required to confirm the generality of the observed small composition shift and its limited impact on cycle performance.

5.5 Future Research

Building upon the findings and the acknowledged limitations of the present study, several ideas for future research are proposed. Firstly, to overcome the ambiguity of some of the presented in-situ measurement approaches, future work could explore multi-sensor integration. Comparing measurements from both a density sensor and a speed of sound sensor simultaneously could provide the extra independent variable needed to distinguish whether a property shift is caused by the varying refrigerant ratio or the presence of circulating oil in the circuit. Furthermore, the refinement of the local composition model could allow the analysis of the impact of oil on the heat transfer mechanisms in the two-phase regions of the heat exchangers. Generally, extra research on the mass and heat transfer resistance, associated with zeotropic mixtures, and enhanced by the presence of oil in the system is necessary. This can play a fundamental role in the proper sizing of heat exchangers when zeotropic mixtures are employed.

6 Conclusion

This study provided a comprehensive experimental and numerical evaluation of the mechanisms driving composition shift in heat pumps using a Propane-Isopentane zeotropic mixture with PAG 68 lubricating oil. The evaluation of different in-situ methods for composition determination highlighted in most cases, the calculated properties showed high sensitivity to the mixture composition, making them appropriate options for detecting composition shift in a given system. The thermodynamic modelling, utilizing the Peng-Robinson EoS and NRTL activity coefficients, quantified the impact of preferential solubility and liquid hold-up. Starting from a nominal composition of 55% Propane/45% Isopentane mass fractions, the preferential solubility of Isopentane in PAG 68 oil, shifted the effective mixture composition to 56.2% Propane/43.8% Isopentane. Furthermore, when accounting for slip effects due to the differences in velocity of the vapour- and liquid-phase, the circulating composition reaches 57.9% Propane/42.1% Isopentane, with approximately 39% of the total charge found to be retained in the heat exchangers (particularly in the evaporator). The cumulative effect of the two investigated mechanisms resulted in a net composition shift of 3.06% in favour of the more volatile component, Propane. The results agree with similar studies investigating the composition shifts of refrigerants mixtures. In terms of system performance, the enrichment of Propane led to an increase of 4.6% in both evaporation and condensation pressures, while the effects on the COP appear to be negligible, with a reduction from 4.34 to 4.31. The VHC calculated with the final circulating composition observes an increase, demonstrating that although the effects on the thermodynamic efficiency is minimal, the composition shift might influence the compressor sizing. Ultimately, this work recognizes the importance of future research on the local heat transfer degradation that may occur due to the composition gradients observed in the two-phase processes, which could result in an increase of heat transfer area due to the decrease in temperature difference during heat transfer mechanisms.

Bibliography

[1] Virginia Natonek. *Thesis-Zeotropic-Mixtures*. URL: https://github.com/virgynatonek/Thesis-Zeotropic-Mixtures.

[2] N. Lakshmi Narasimhan and G. Venkatarathnam. "A method for estimating the composition of the mixture to be charged to get the desired composition in circulation in a single stage JT refrigerator operating with mixtures". In: *Cryogenics* 50.2 (Feb. 2010), pp. 93–101. ISSN: 0011-2275. DOI: 10.1016/J.CRYOGENICS.2009.12.004. URL: https://www.sciencedirect.com/science/article/pii/S0011227509002045?via%3Dihub.

[3] Muhammad Haider and Stefan Elbel. "Methods of measuring circulation composition for zeotropic binary mixture refrigerants". In: *International Journal of Refrigeration* 177 (Sept. 2025), pp. 232–243. ISSN: 0140-7007. DOI: 10.1016/J.IJREFRIG.2025.05.022. URL: https://www.sciencedirect.com/science/article/pii/S0140700725002105.

[4] Leon P.M. Brendel et al. "High-glide refrigerant blends in high-temperature heat pumps: Part 2 – Inline composition determination for binary mixtures". In: *International Journal of Refrigeration* 165 (Sept. 2024), pp. 45–57. ISSN: 0140-7007. DOI: 10.1016/J.IJREFRIG.2024.05.012. URL: https://www.sciencedirect.com/science/article/pii/S0140700724001610.

[5] Junjiang Bao and Li Zhao. "Experimental research on the influence of system parameters on the composition shift for zeotropic mixture (isobutane/pentane) in a system occurring phase change". In: *Energy Conversion and Management* 113 (Apr. 2016), pp. 1–15. ISSN: 0196-8904. DOI: 10.1016/J.ENCONMAN.2016.01.017. URL: https://www.sciencedirect.com/science/article/pii/S0196890416000339.

[6] P. Haberschill et al. "Performance prediction of a refrigerating machine using R-407C: The effect of the circulating composition on system performance". In: *International Journal of Energy Research* 26.15 (Dec. 2002), pp. 1295–1311. ISSN: 0363907X. DOI: 10.1002/er.817. URL: https://www.scopus.com/pages/publications/0036926902.

[7] Ju Hyok Kim et al. "Circulation concentration of CO2/propane mixtures and the effect of their charge on the cooling performance in an air-conditioning system". In: *International Journal of Refrigeration* 30.1 (Jan. 2007), pp. 43–49. ISSN: 0140-7007. DOI: 10.1016/J.IJREFRIG.2006.06.008. URL: https://www.sciencedirect.com/science/article/pii/S0140700706001393.

[8] Jean-Marc Lebreton and Louis Vuillame. "Oil Concentration Measurement In Saturated Liquid Refrigerant Flowing Inside A Refrigeration Machine". In: *Int. J. Applied Thermodynamics* 4.1 (Mar. 2001), pp. 53–60. URL: https://www.researchgate.net/publication/42539792_Oil_Concentration_Measurement_In_Saturated_Liquid_Refrigerant_Flowing_Inside_A_Refrigeration_Machine.

[9] Y. Mermond, M. Feidt, and C. Marvillet. "Propriétés thermodynamiques et physiques des mélanges de fluides frigorigènes et d'huiles". In: *International Journal of Refrigeration* 22.7 (Nov. 1999), pp. 569–579. ISSN: 0140-7007. DOI: 10.1016/S0140-7007(99)00015-8. URL: https://www.sciencedirect.com/science/article/pii/S0140700799000158.

[10] Leelananda Rajapaksha. "Influence of special attributes of zeotropic refrigerant mixtures on design and operation of vapour compression refrigeration and heat pump systems". In: *Energy Conversion and Management* 48.2 (Feb. 2007), pp. 539–545. ISSN: 0196-8904. DOI: 10.1016/J.ENCONMAN.2006.06.001. URL: https://www.sciencedirect.com/science/article/pii/S0196890406001993.

[11] S Corr, F T Murphy, and S Wilkinson. “Composition shifts of zeotropic HFC refrigerants in service”. In: (Dec. 1994). ISSN: 0001-2505.

[12] J. Chen and H. Kruse. “Calculating circulation concentration of zeotropic refrigerant mixtures”. In: *HVAC and R Research* 1.3 (1995), pp. 219–231. ISSN: 10789669. DOI: 10.1080/10789669.1995.10391320;ISSUE:ISSUE:DOI. URL: https://www.tandfonline.com/doi/abs/10.1080/10789669.1995.10391320.

[13] William E. Vaughan and Frank C. Collins. “P-V-T-x Relations of the System Propane-Isopentane”. In: *Industrial & Engineering Chemistry* 34.7 (July 2002), pp. 885–890. ISSN: 0019-7866. DOI: 10.1021/IE50391A027. URL: https://pubs.acs.org/doi/abs/10.1021/ie50391a027.

[14] *RENISO PG 68 | Refrigeration oil*. URL: https://www.fuchs.com/de/en/product/product/148775-reniso-pg-68/.

[15] *SYNDUSTRIAL® PAG COMPRESSOR OIL - Phillips 66 Lubricants*. URL: https://www.phillips66lubricants.com/product/syndustrial-pag-compressor-oil/.

[16] Manuel R. Conde. “Estimation of thermophysical properties of lubricating oils and their solutions with refrigerants: An appraisal of existing methods”. In: *Applied Thermal Engineering* 16.1 (Jan. 1996), pp. 51–61. ISSN: 1359-4311. DOI: 10.1016/1359-4311(95)00011-2. URL: https://www.sciencedirect.com/science/article/pii/1359431195000112.

[17] Yanjun Sun et al. “Oil solubility effect on evaporation performance with R290 as refrigerant”. In: *International Journal of Refrigeration* 151 (July 2023), pp. 200–207. ISSN: 0140-7007. DOI: 10.1016/J.IJREFRIG.2023.04.007. URL: https://www.sciencedirect.com/science/article/pii/S0140700723001007.

[18] Eric W. Lemmon, Marcia L. Huber, and Mark O. McLinden. *NIST Standard Reference Database 23: Reference Fluid Thermodynamic and Transport Properties-REFPROP, Version 9.1*. Tech. rep. 2013. URL: https://www.nist.gov/publications/nist-standard-reference-database-23-reference-fluid-thermodynamic-and-transport.

[19] Ji Zhang, Brian Elmegaard, and Fredrik Haglind. “Condensation heat transfer and pressure drop characteristics of zeotropic mixtures of R134a/R245fa in plate heat exchangers”. In: *International Journal of Heat and Mass Transfer* 164 (Jan. 2021), p. 120577. ISSN: 0017-9310. DOI: 10.1016/J.IJHEATMASSTRANSFER.2020.120577. URL: https://www.sciencedirect.com/science/article/pii/S0017931020335134.

[20] *Speed of sound measurements in gas-mixtures at varying composition using an ultrasonic gas flow meter with silicon based transducers*. URL: https://www.researchgate.net/publication/235330318_Speed_of_sound_measurements_in_gas-mixtures_at_varying_composition_using_an_ultrasonic_gas_flow_meter_with_silicon_based_transducers.

[21] A. Johansson and P. Lundqvist. “A method to estimate the circulated composition in refrigeration and heat pump systems using zeotropic refrigerant mixtures”. In: *International Journal of Refrigeration* 24.8 (Dec. 2001), pp. 798–808. ISSN: 0140-7007. DOI: 10.1016/S0140-7007(00)00061-X. URL: https://www.sciencedirect.com/science/article/pii/S014070070000061X.

[22] Robert J. Moffat. “Describing the uncertainties in experimental results”. In: *Experimental Thermal and Fluid Science* 1.1 (Jan. 1988), pp. 3–17. ISSN: 0894-1777. DOI: 10.1016/0894-1777(88)90043-X. URL: https://www.sciencedirect.com/science/article/pii/089417778890043X?via%3Dihub.

[23] S. Kline. “Describing Uncertainties in Single-Sample Experiments”. In: *Mechanical Engineering* (1953).

[24] Mohammed Youbi-Idrissi and Jocelyn Bonjour. “The effect of oil in refrigeration: Current research issues and critical review of thermodynamic aspects”. In: *Inter-*

national Journal of Refrigeration 31.2 (Mar. 2008), pp. 165–179. ISSN: 0140-7007. DOI: 10.1016/J.IJREFRIG.2007.09.006. URL: https://www.sciencedirect.com/science/article/pii/S0140700707001867.

[25] Åsa Wahlström and Lennart Vamling. "Solubility of HFC32, HFC125, HFC134a, HFC143a, and HFC152a in a pentaerythritol tetrapentanoate ester". In: *Journal of Chemical and Engineering Data* 44.4 (July 1999), pp. 823–828. ISSN: JCEAAX. DOI: 10.1021/JE980235E.

[26] Mahmood Moshfeghian, Ahmad Shariat, and Robert N. Maddox. "Prediction of refrigerant thermodynamic properties by equations of state: vapor liquid equilibrium behavior of binary mixtures". In: *Fluid Phase Equilibria* 80.C (Nov. 1992), pp. 33–44. ISSN: 0378-3812. DOI: 10.1016/0378-3812(92)87053-P. URL: https://www.sciencedirect.com/science/article/pii/037838129287053P.

[27] Chung Tong Lin and Thomas E. Daubert. "Estimation of Partial Molar Volume and Fugacity Coefficient of Components in Mixtures from the Soave and Peng-Robinson Equations of State". In: *Industrial and Engineering Chemistry Process Design and Development* 19.1 (Jan. 2002), pp. 51–59. ISSN: 01964305. DOI: 10.1021/I260073A009. URL: /doi/pdf/10.1021/i260073a009?ref=article_openPDF.

[28] W. L. Martz, C. M. Burton, and A. M. Jacobi. "Local composition modelling of the thermodynamic properties of refrigerant and oil mixtures". In: *International Journal of Refrigeration* 19.1 (Jan. 1996), pp. 25–33. ISSN: 0140-7007. DOI: 10.1016/0140-7007(95)00063-1. URL: https://www.sciencedirect.com/science/article/pii/0140700795000631.

[29] Ding Yu Peng and Donald B. Robinson. "A New Two-Constant Equation of State". In: *Industrial and Engineering Chemistry Fundamentals* 15.1 (1976), pp. 59–64. ISSN: 01964313. DOI: 10.1021/I160057A011.

[30] P. Guillemet and O. Lottin. "Modélisation des équilibres liquide–vapeur, application aux mélanges d'huile et de fluides frigorigènes HFC". In: *International Journal of Refrigeration* 27.2 (Mar. 2004), pp. 102–110. ISSN: 0140-7007. DOI: 10.1016/J.IJREFRIG.2003.09.004. URL: https://www.sciencedirect.com/science/article/pii/S0140700703001361.

[31] ASHRAE. "ASHRAE Handbook of Fundamentals. Atlanta: American Society of Heating Refrigerating and Air conditioning Engineers". In: *ASHRAE handbook series* (1997), p. 851. URL: https://www.worldcat.org/title/1997-ashrae-handbook-fundamentals/oclc/37607716.

[32] H.C. VAN NESS. "APPLICATIONS TO VAPOR–LIQUID EQUILIBRIUM". In: *Classical Thermodynamics of Non-Electrolyte Solutions* (1964), pp. 111–150. DOI: 10.1016/B978-1-4832-0044-6.50009-8.

[33] Seif Eddeen K. Fateen, Menna M. Khalil, and Ahmed O. Elnabawy. "Semi-empirical correlation for binary interaction parameters of the Peng–Robinson equation of state with the van der Waals mixing rules for the prediction of high-pressure vapor–liquid equilibrium". In: *Journal of Advanced Research* 4.2 (Mar. 2013), pp. 137–145. ISSN: 2090-1232. DOI: 10.1016/J.JARE.2012.03.004. URL: https://www.sciencedirect.com/science/article/pii/S2090123212000264.

[34] Dimitrios P. Tassios. "Applied Chemical Engineering Thermodynamics". In: *Applied Chemical Engineering Thermodynamics* (1993). DOI: 10.1007/978-3-662-01645-9.

[35] C. Burton, A. M. Jacobi, and S. S. Mehendale. "Vapor-liquid equilibrium for R-32 and R-410A mixed with a polyol ester: non-ideality and local composition modeling". In: *International Journal of Refrigeration* 22.6 (Sept. 1999), pp. 458–471. ISSN: 0140-7007. DOI: 10.1016/S0140-7007(99)00012-2. URL: https://www.sciencedirect.com/science/article/pii/S0140700799000122.

[36] J. S. Fleming and Y. Yan. “The prediction of vapour–liquid equilibrium behaviour of HFC blend–oil mixtures from commonly available data”. In: *International Journal of Refrigeration* 26.3 (May 2003), pp. 266–274. ISSN: 0140-7007. DOI: 10.1016/S0140-7007(02)00130-5. URL: https://www.sciencedirect.com/science/article/pii/S0140700702001305.

[37] WILSON G. M. “A New Expression for the Excess Free Energy of Mixing”. In: *J. Am. Chem. Soc.* 86 (1964), pp. 127–. URL: https://cir.nii.ac.jp/crid/1570009749753077120.

[38] J. F. Heil and J. M. Prausnitz. “Phase equilibria in polymer solutions”. In: *AIChE Journal* 12.4 (July 1966), pp. 678–685. ISSN: 15475905. DOI: 10.1002/AIC.690120412;JOURNAL:JOURNAL:15475905;PAGEGROUP:STRING:PUBLICATION. URL: /doi/pdf/10.1002/aic.690120412%20https://onlinelibrary.wiley.com/doi/abs/10.1002/aic.690120412%20https://aiche.onlinelibrary.wiley.com/doi/10.1002/aic.690120412.

[39] Wenchuan Wang and Kwang Chu Chao. “The complete local concentration model activity coefficients”. In: *Chemical Engineering Science* 38.9 (Jan. 1983), pp. 1483–1492. ISSN: 0009-2509. DOI: 10.1016/0009-2509(83)80083-9. URL: https://www.sciencedirect.com/science/article/pii/0009250983800839.

[40] Takeshi Tsuboka and Takashi Katayama. “MODIFIED WILSON EQUATION FOR VAPOR-LIQUID AND LIQUID-LIQUID EQUILIBRIA”. In: *JOURNAL OF CHEMICAL ENGINEERING OF JAPAN* 8.3 (June 1975), pp. 181–187. ISSN: 0021-9592. DOI: 10.1252/JCEJ.8.181.

[41] Henri Renon and J. M. Prausnitz. “Local compositions in thermodynamic excess functions for liquid mixtures”. In: *AIChE Journal* 14.1 (Jan. 1968), pp. 135–144. ISSN: 15475905. DOI: 10.1002/AIC.690140124;ISSUE:ISSUE:DOI. URL: /doi/pdf/10.1002/aic.690140124%20https://onlinelibrary.wiley.com/doi/abs/10.1002/aic.690140124%20https://aiche.onlinelibrary.wiley.com/doi/10.1002/aic.690140124.

[42] Edward Armand Guggenheim. *Mixtures: The Theory of the Equilibrium Properties of Some Simple Classes of Mixtures, Solution and Alloys*. 1952. URL: https://books.google.dk/books/about/Mixtures.html?id=1tXQAAAAMAAJ&redir_esc=y.

[43] Norman Silverman and Dimitrios Tasslos. “Prediction of multicomponent vapor-liquid equilibrium with the Wilson equation: effect of the minimization function and of the quality of binary data”. In: *Ind. Eng. Chem. Process Des. Dev.; (United States)* 23:3.3 (July 1984), pp. 586–589. ISSN: IEPDA. DOI: 10.1021/I200026A030.

[44] J J Grebner and R R Crawford. “The Effects of Oil on the Thermodynamic Properties of Dichlorodifluoromethane (R-12) and Tetrafluoroethane (R-134a)”. In: *Air Conditioning and Refrigeration Center TR-13* (1992). URL: https://hdl.handle.net/2142/9702%20http://hdl.handle.net/2142/9702.

[45] J.R. Thome. “Comprehensive thermodynamic approach to modelling refrigerant-lubricating oil mixtures.” In: *HVAC&R Research* 1.2 (Apr. 1995). URL: https://iifiir.org/en/fridoc/comprehensive-thermodynamic-approach-to-modelling-103551.

[46] Xiongwen Xu et al. “Local composition shift of mixed working fluid in gas–liquid flow with phase transition”. In: *Applied Thermal Engineering* 39 (June 2012), pp. 179–187. ISSN: 1359-4311. DOI: 10.1016/J.APPLTHERMALENG.2012.01.064. URL: https://www.sciencedirect.com/science/article/pii/S1359431112000932.

[47] Yeonwoo Jeong, Sangwook Lee, and Min Soo Kim. “Local composition shift of refrigerant mixtures and its effect on cooling performance in a heat pump system”. In: *Energy Conversion and Management* 333 (June 2025), p. 119809. ISSN: 0196-8904. DOI: 10.1016/J.ENCONMAN.2025.119809. URL: https://www.sciencedirect.com/science/article/abs/pii/S0196890425003322.

[48] M. Youbi-Idrissi, J. Bonjour, and F. Meunier. “Local shifts of the fluid composition in a simulated heat pump using R-407C”. In: *Applied Thermal Engineering* 25.17-18

(Dec. 2005), pp. 2827–2841. ISSN: 1359-4311. DOI: 10.1016/J.APPLTHERMALENG.2005.02.005. URL: https://www.sciencedirect.com/science/article/abs/pii/S1359431105000669.

[49] Li Zhao and Junjiang Bao. "The influence of composition shift on organic Rankine cycle (ORC) with zeotropic mixtures". In: *Energy Conversion and Management* 83 (July 2014), pp. 203–211. ISSN: 0196-8904. DOI: 10.1016/J.ENCONMAN.2014.03.072. URL: https://www.sciencedirect.com/science/article/pii/S0196890414002830.

[50] SMITH SL. "Void fractions in two- phase flow. A correlation based upon an equal velocity head model". In: *Proceedings of the Institution of Mechanical Engineers* 18 (1969), pp. 647–664. ISSN: 0020-3483. DOI: 10.1243/PIME{_}PROC{_}1969{_}184{_}051{_}02;WEBSITE:WEBSITE:SAGE;JOURNAL:JOURNAL:PMEA;ISSUE:ISSUE:DOI. URL: /doi/pdf/10.1243/PIME_PROC_1969_184_051_02?download=true.

[51] John. Prausnitz et al. "Molecular Thermodynamics of Fluid-Phase Equilibria". In: (1998), p. 896. URL: https://books.google.com/books/about/Molecular_Thermodynamics_of_Fluid_Phase.html?id=VSwc1XUmYpcC.

[52] Yaodong Zhou, Fengyuan Zhang, and Lijun Yu. "The discussion of composition shift in organic Rankine cycle using zeotropic mixtures". In: *Energy Conversion and Management* 140 (May 2017), pp. 324–333. ISSN: 0196-8904. DOI: 10.1016/J.ENCONMAN.2017.02.081. URL: https://www.sciencedirect.com/science/article/pii/S0196890417301929.

[53] Zhaohua Li et al. "A numerical study on the effect of oil lubricant on the heat transfer and efficiency of a vapour compression refrigeration system". In: *International Communications in Heat and Mass Transfer* 134 (May 2022), p. 106016. ISSN: 0735-1933. DOI: 10.1016/J.ICHEATMASSTRANSFER.2022.106016. URL: https://www.sciencedirect.com/science/article/pii/S0735193322001385.

[54] Predrag Popovic. "Investigation and analysis of lubricant effects on the performance of an HFC-134a refrigeration system". In: (1999). DOI: 10.31274/RTD-180813-13744. URL: https://lib.dr.iastate.edu/rtd/12476/.

A Appendix

A.1 Data used for NRTL-based model

Table A.1: Solubilities of Propane in PAG 68 oil [17].

T/K	p/MPa	x_1	T/K	p/MPa	x_1
283.15	0.150	0.272	313.15	0.839	0.607
283.15	0.322	0.493	313.15	1.043	0.703
283.15	0.470	0.657	313.15	1.224	0.791
283.15	0.580	0.779	323.15	0.193	0.167
283.15	0.625	0.861	323.15	0.427	0.325
283.15	0.627	0.909	323.15	0.662	0.455
293.15	0.162	0.238	323.15	0.900	0.560
293.15	0.352	0.442	323.15	1.133	0.651
293.15	0.530	0.597	323.15	1.360	0.733
293.15	0.685	0.721	333.15	0.202	0.151
293.15	0.790	0.819	333.15	0.449	0.297
293.15	0.822	0.888	333.15	0.699	0.418
303.15	0.173	0.210	333.15	0.955	0.520
303.15	0.380	0.396	333.15	1.211	0.606
303.15	0.579	0.543	333.15	1.470	0.684
303.15	0.770	0.662	343.15	0.211	0.138
303.15	0.933	0.762	343.15	0.469	0.274
303.15	1.040	0.848	343.15	0.733	0.389
313.15	0.183	0.186	343.15	1.006	0.485
313.15	0.405	0.358	343.15	1.282	0.568
313.15	0.623	0.496	343.15	1.568	0.643

Table A.2: VLE data of the Propane-Isopentane mixture at different temperatures.

T/K	p/MPa	x_1
313.0	0.217	0.05
313.0	0.342	0.15
313.0	0.460	0.25
313.0	0.574	0.35
313.0	0.687	0.45
313.0	0.801	0.55
313.0	0.917	0.65
313.0	1.037	0.75
313.0	1.161	0.85
313.0	1.294	0.95
323.0	0.284	0.05
323.0	0.434	0.15
323.0	0.577	0.25
323.0	0.717	0.35
323.0	0.856	0.45
323.0	0.998	0.55
323.0	1.142	0.65
323.0	1.291	0.75
323.0	1.448	0.85
323.0	1.617	0.95
333.0	0.365	0.05
333.0	0.543	0.15
333.0	0.714	0.25
333.0	0.883	0.35
333.0	1.053	0.45
333.0	1.225	0.55
333.0	1.403	0.65
333.0	1.587	0.75
333.0	1.782	0.85
333.0	1.994	0.95

A.2 Verification and Validation of the Local Composition Models

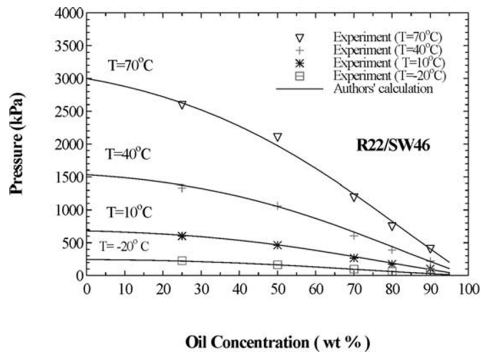

(a) Authors' calculation from the literature [36].

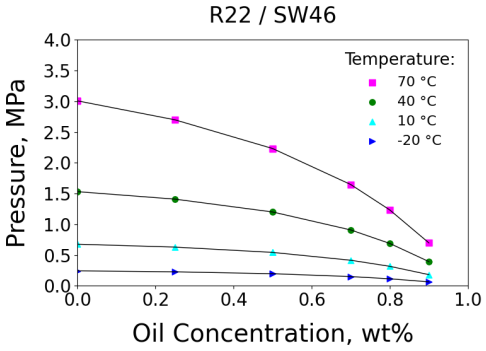

(b) Present PR–NRTL-based model.

Figure A.1: Comparison of pressure–oil concentration relationships for the R R22/SW46 system obtained from literature data (a) and the present model (b).

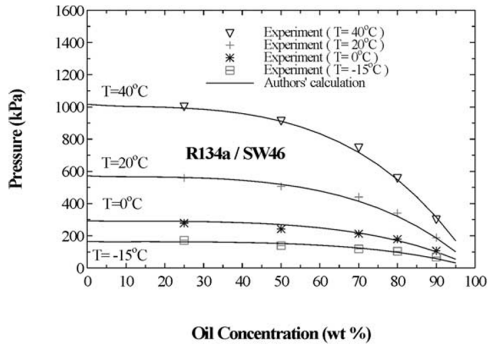

(a) Authors' calculation from the literature [36].

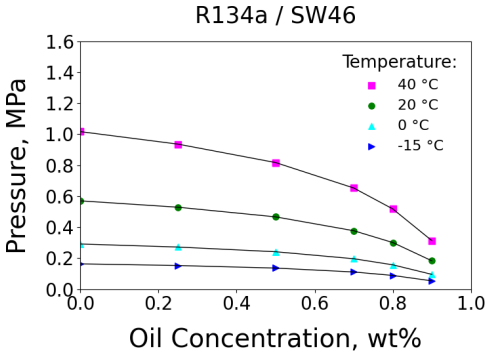

(b) Present PR–NRTL-based model.

Figure A.2: Comparison of pressure–oil concentration relationships for the R R134a/SW46 system obtained from literature data (a) and the present model (b).

Technical
University of
Denmark

Brovej, Building 404
2800 Kgs. Lyngby
Tlf. 4525 1700

www.construct.dtu.dk